Opto-Electronic Technology

CN 51-1811/O4 ISSN (Print) 2097-6003 ISSN (Online) 2097-8006

High-speed and large-capacity visible light communication for 6G: advances and perspectives

Nan Chi*, Zhilan Lu, Fujie Li, Haoyu Zhang, Yunkai Wang, Xinyi Liu, Zhiwu Chen, Zhe Feng, Zhuoran Hu, Zhixue He, Ziwei Li, Chao Shen and Junwen Zhang

Citation: Chi N, Lu ZL, Li FJ, Zhang HY, Wang YK, Liu XY, Chen ZW, Feng Z, Hu ZR, He ZX, Li ZW, Shen C, Zhang JW. High-speed and large-capacity visible light communication for 6G: advances and perspectives. *Opto-Electron Technol* **2**, 260004 (2026).

https://doi.org/10.29026/oet.2026.260004

Received: 31 January 2026; Accepted: 19 March 2026; Published online: 30 March 2026

Related articles

OET Opto-Electronic Technology

Review

March 2026, Vol. 2, No. 1

Open Access

High-speed and large-capacity visible light communication for 6G: advances and perspectives

Nan Chi[1,2,3]*, Zhilan Lu[1], Fujie Li[1], Haoyu Zhang[1], Yunkai Wang[1], Xinyi Liu[1], Zhiwu Chen[1], Zhe Feng[1], Zhuoran Hu[1], Zhixue He[4], Ziwei Li[1], Chao Shen[1] and Junwen Zhang[1]

Abstract: The sixth generation (6G) of mobile communications aims to establish high-speed, large-capacity space-air-ground-sea integrated networks (SAGSINs) to support the rapidly growing data traffic driven by big data and large-scale artificial intelligence. Visible light communication (VLC), operating in the 380–780 nm spectrum, has emerged as a promising optical wireless technology owing to its abundant spectral resources, high achievable data rates, and immunity to electromagnetic interference. These advantages make VLC a strong candidate for three-dimensional integrated communication networks. This review summarizes recent advances in visible light communication, focusing on key enabling technologies including transmitter and receiver devices, advanced signal processing algorithms, multi-aperture reception, and beamforming techniques. Representative demonstrations of large-capacity VLC systems based on multi-dimensional multiplexing are reviewed. Finally, the challenges and future research directions of VLC are discussed.

Keywords: visible light communication; high-speed; large-capacity

DOI: 10.29026/oet.2026.260004 | CSTR: 32419.14.oet.2026.260004

Citation: Chi N, Lu ZL, Li FJ et al. High-speed and large-capacity visible light communication for 6G: advances and perspectives. *Opto-Electron Technol* **2**, 260004 (2026).

1 Introduction

Communication networks are evolving from conventional information exchange platforms into infrastructures that connect everything and enable intelligence. The explosive growth of data-intensive applications, such as 4K/8K video streaming, augmented and virtual reality, the Internet of Things (IoT), artificial intelligence, and digital twins, has resulted in traffic demands several orders of magnitude higher than those of traditional text and voice services[1,2]. To address these challenges, sixth-generation mobile communication (6G) proposes the construction of high-speed, large-capacity space-air-ground-sea integrated networks (SAGSINs). A fundamental objective of 6G is to achieve a substantial increase in peak transmission capacity. However, the scarcity of radio-frequency spectrum limits further capacity expansion using conventional technologies. Consequently, disruptive approaches such as massive multiple-input multiple-output (MIMO) and the exploitation of higher-frequency bands, including millimeter-wave, terahertz, and visible light, have attracted significant attention[3,4].

The visible light spectrum, from 380 nm to 780 nm, provides a spectral resources approximately four orders of magnitude larger than those of commonly used wireless bands, making it a promising complement to existing communication technologies. Visible light communication (VLC) offers several intrinsic advantages, including energy efficiency, high security, resistance to electromagnetic interference, and high signal-to-noise ratio (SNR), enabling high-speed data transmission[5–7]. In recent years, the technological trajectory of VLC has gradually shifted from the conventional communication-illumination integration paradigm toward positioning the visible spectrum as an independent carrier for high-speed data transmission. Early VLC systems were predominantly built upon light emitting diode (LED) lighting infrastructures, where data signals

Received: 31 January 2026
Accepted: 19 March 2026
Published online: 30 March 2026

[1]Key Laboratory for the Information Science of Electromagnetic Waves (MoE), College of Future Information Technology, Fudan University, Shanghai 200433, China; [2]Shanghai Engineering Research Center of Low-Earth-Orbit Satellite Communication and Applications, Shanghai 200433, China; [3]Shanghai Collaborative Innovation Center of Low-Earth-Orbit Satellite Communication Technology, Shanghai 200433, China; [4]Peng Cheng Laboratory, Shenzhen 518055, China.
*Correspondence: N Chi, E-mail: nanchi@fudan.edu.cn

were superimposed onto illumination sources. As a result, system design had to strictly comply with lighting standards, including illuminance, correlated color temperature, and flicker mitigation. In addition, indoor mobile scenarios were particularly susceptible to link interruptions caused by human movement or object blockage. Driven by the emerging requirements of large capacity, ultra-high data rates, and cable-free connectivity in 6G networks, current research has increasingly focused on breakthroughs in high-speed transmission, multidimensional multiplexing techniques, and massively parallel architectures. Correspondingly, system implementations are evolving from general-purpose lighting LEDs toward high-bandwidth laser-based transmitters[8]. These configurations are primarily intended for dedicated scenarios such as data center interconnects, underwater directional links, and inter-satellite communications, where illumination functionality is not required. Instead, link design emphasizes line-of-sight transmission and precise alignment, rendering the overall technical framework closer to that of free-space optical communication systems. Under such conditions, the dependence on conventional lighting standards is substantially reduced, and blockage issues associated with diffuse illumination structures become less critical. Industrial developments further reflect this transition. For instance, companies such as Avicena are actively advancing high-speed visible light interconnect technologies[9–11], aiming to establish communication platforms characterized by high bandwidth, low power consumption, and scalable architectures. In this context, recent research efforts have concentrated on key devices, signal processing algorithms, and system architectures that enable high-speed, large-capacity transmission with parallel scalability. It should be noted that when VLC systems are implemented on public lighting infrastructures, their design must comply with relevant national and international lighting engineering standards, including requirements on illuminance levels, color rendering performance, and flicker safety. These constraints may limit parameters such as modulation depth and optical power allocation in practical system implementations. In contrast, in emerging application scenarios such as data-center optical interconnects, underwater wireless optical communications, and inter-satellite or satellite-to-ground links, optical sources typically operate as dedicated communication transmitters rather than illumination devices. Consequently, system design in these contexts is primarily driven by communication performance requirements, while the dependence on conventional lighting engineering standards becomes significantly less critical.

Given the aforementioned characteristics and development trends, VLC aligns well with several key requirements of 6G networks, including high energy efficiency, strong reliability, and ubiquitous connectivity, thereby exhibiting significant application potential. As illustrated in Fig. 1, VLC is expected to play an important role in next-generation three-dimensional communication networks. In space-based networks, VLC benefits from the radiation tolerance of third-generation wide-bandgap semiconductors and the favorable characteristics of laser sources, such as short wavelengths, long transmission distances, and high output power, making it suitable for inter-satellite communication links[12,13]. In maritime environments, the blue-green region of the visible spectrum coincides with the underwater transmission window, enabling underwater VLC systems with high data rates, large capacity, and low latency[14,15]. In data center optical interconnects, VLC meets the stringent requirements for low latency and large-scale data exchange, showing considerable application potential[16–18]. For indoor access, its license-free operation, cost-effectiveness, and inherent security make VLC a competitive candidate technology[19,20]. Moreover, the high-speed and flexible nature of VLC enables vehicle-to-everything (V2X) communications, supporting autonomous driving and intelligent transportation systems[21].

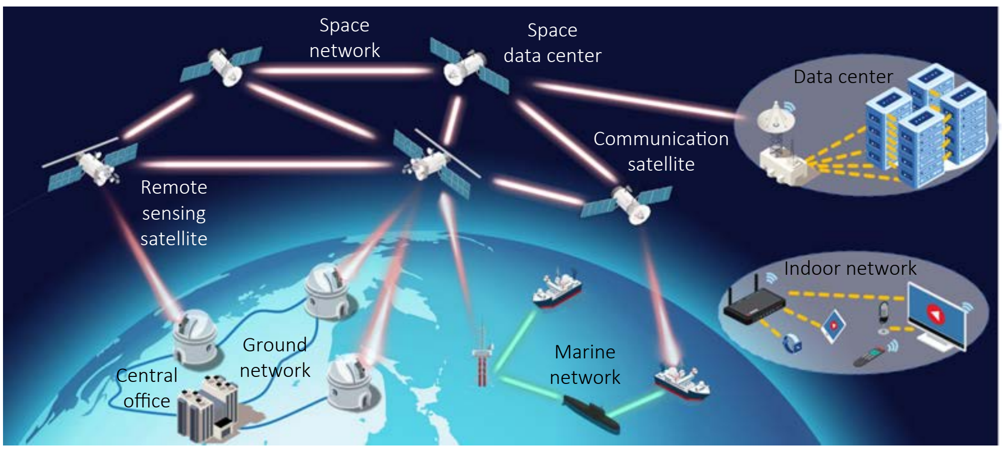

Fig. 1 | Applications of visible light communication in space, ground, underwater, data center and indoor networks.

In addition, channel characteristics, deployment configurations, and system constraints vary substantially across different application scenarios, which implies that the development of VLC technologies should be application-oriented and context-specific. Consequently, it is essential to examine representative scenarios individually, identify their core technical requirements, and clarify the corresponding enabling approaches. Table 1 summarizes the typical applications and associated technical demands under different scenarios[13,22,23].

However, VLC systems face inherent challenges associated with intensity modulation and direct detection (IMDD), including limited modulation bandwidth, low spectral efficiency, device nonlinearity, and inefficient channel multiplexing. The transmission theory, channel models, and processing methods of traditional optical communication systems cannot be directly applied to high-speed VLC systems. As shown in Fig. 2, addressing these challenges requires coordinated advances in broadband device development, efficient signal processing, and large-capacity system architectures. Over the past decades, extensive research efforts have led to significant progress across these dimensions. Representative achievements in VLC are summarized in Fig. 3, demonstrating continuous improvements in transmission speed, distance, and capacity[16, 24–61]. In device development, efforts primarily focus on enhancing the bandwidth of transmitters and detectors, as well as improving the photoelectric effect. Signal processing research concentrates on increasing the linearity of transmitted signals and mitigating both linear and nonlinear channel distortions. However, data rate improvements in single-wavelength, single-channel systems have been relatively gradual. To achieve a substantial capacity increase, system and network level optimization is essential. Although the highest reported data rate for point-to-point (P2P) VLC systems is 36.5 Gbps[44], multi-wavelength systems employing multi-dimensional multiplexing have demonstrated clear advantages. Experimental VLC systems exceeding 600 Gbps and even 800 Gbps have been successfully demonstrated[16,43].

From the perspective of capacity scaling, this paper systematically reviews the coordinated advances in devices, algorithms, and system architectures that enable high-speed VLC, with particular emphasis on large-capacity transmission and multidimensional parallel architectures. Table 2 compares the main focus of representative VLC review papers published over the past five years[5,8,62–69]. Most existing VLC surveys summarize the field from a single perspective, such as device technologies, modulation and signal processing techniques, or specific application scenarios. However, a systematic analysis centered on capacity scaling mechanisms remains relatively limited. In contrast, motivated by the large-capacity and high-speed transmission requirements envisioned for 6G, this paper reconstructs and analyzes recent progress in VLC from the perspective of capacity enhancement mechanisms. Through this capacity-driven and system-oriented analytical framework, this work

Table 1 | Typical applications and associated technical demands of different scenarios.

Scenario	Representative applications	Required technical enablers	Corresponding sections
Space network	Inter-satellite optical links, low earth orbit communication, deep-space communication	High-directionality transmitters, high-sensitivity receivers, robust channel estimation, beam steering	Transmitters, receivers, channel estimation, beamforming
Ground network	Smart cities, vehicular networks intelligent transportation systems	Wide-FOV receivers, adaptive modulation, pre/post-equalization, multi-aperture receiver	Receivers, coding and modulation, pre/post-equalization, multi-aperture receiver
Marine network	Underwater sensor networks, autonomous underwater vehicle (AUV) communication	Blue-green transmitters, high-sensitivity receivers, robust channel estimation, multi-aperture receiver	Transmitters, receivers, channel estimation, multi-aperture receiver
Data center	Rack-to-rack interconnects, board-level optical wireless links	High-bandwidth transceiver, high-order modulation, beam steering, large-capacity transmission	Transmitters, receivers, coding and modulation, beamforming, large-capacity system
Indoor network	Augmented reality, virtual reality, industrial IoT	Multi-user modulation, adaptive equalization, beam steering	Coding and modulation, post-equalization, beamforming

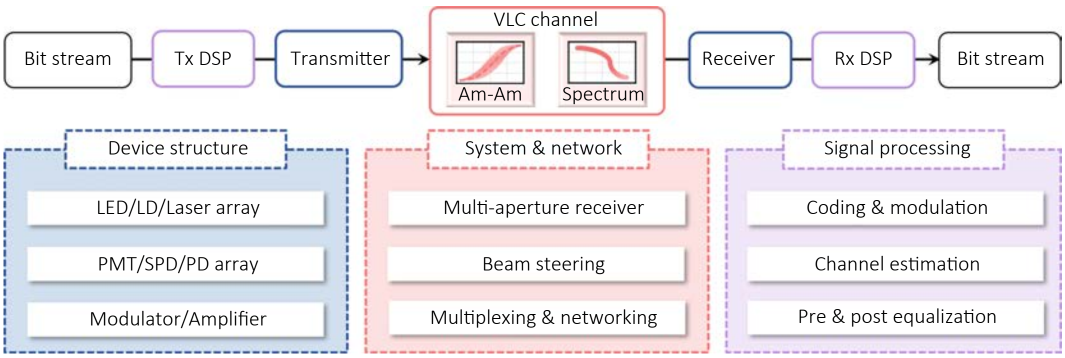

Fig. 2 | The enabling technologies in VLC system including devices, algorithms and system architectures.

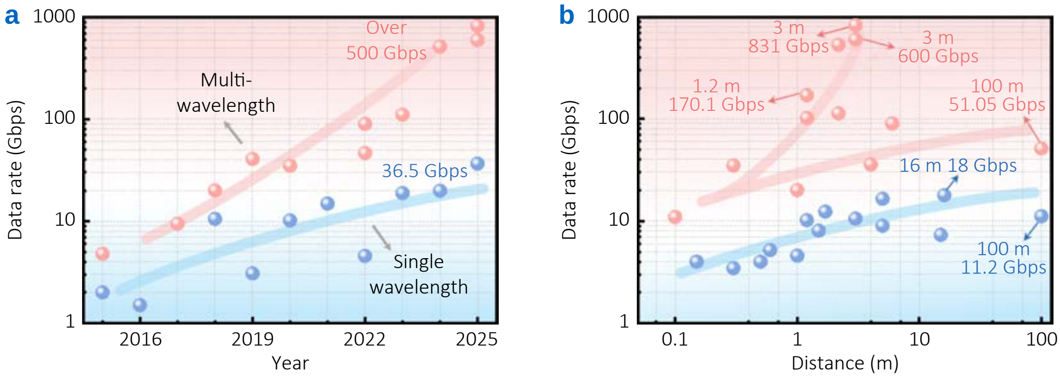

Fig. 3 | Recent achievements of high-speed VLC systems.

Table 2 | Comparison of representative VLC review papers published in the past five years.

Ref.	Year	Primary focus	Device	Algorithm	Multi-dimensional multiplexing	Large-capacity system
62	2022	VLC for IoT	Partial	Partial	Limited	Limited
63	2022	GaN laser diode	Comprehensive	Not mentioned	Not mentioned	Not mentioned
64	2023	Machine learning	Not mentioned	Comprehensive	Not mentioned	Partial
65	2023	Transceiver of VLC	Comprehensive	Limited	Limited	Partial
66	2023	MIMO VLC	Limited	Comprehensive	Partial	Partial
8	2023	Large-capacity demonstration	Partial	Partial	Partial	Comprehensive
67	2024	Integrated sensing, lighting and communication	Partial	Partial	Limited	Limited
5	2024	Underwater VLC	Partial	Partial	Limited	Limited
68	2025	VLC in transportation systems	Partial	Partial	Partial	Limited
69	2025	Underwater VLC	Partial	Partial	Not mentioned	Limited
This paper	2026	Large-capacity VLC for 6G	Comprehensive	Comprehensive	Comprehensive	Comprehensive

aims to provide a clear technological roadmap for the design and large-scale deployment of high-speed VLC systems in future 6G communication networks.

2 Key VLC devices: transmitters and receivers

Visible light communication systems primarily rely on two key components: optical transmitters and photodetectors. Performance improvements at the device level mainly focus on extending modulation bandwidth and enhancing efficiency through structural engineering, such as quantum wells, V-pits, and cavity optimization. In addition, array-based devices play an increasingly important role in boosting system capacity and integration density.

2.1 Bandwidth-enhanced transmitters

LEDs and laser diodes (LDs) constitute the primary optical transmitters employed in VLC systems. LEDs operate based on the spontaneous emission mechanism of semiconductor PN junctions, where signals are transmitted by directly modulating the optical intensity via injection current. They offer advantages such as low cost and excellent compatibility with existing lighting infrastructure. To overcome the modulation bandwidth limitations of traditional LEDs, research has shifted toward size miniaturization, structural innovation and array configurations. Li et al. optimized the mesa size and single-layer InGaN active region to fabricate a 150 μm blue mini-LED with a bandwidth of 906 MHz[70], achieving a transmission rate of 4 Gbps. For Micro-LEDs, Li et al. incorporated InGaN quantum dots and formulated an equivalent circuit model to quantitatively decouple the bandwidth constraints imposed by resistor-capacitance (RC) time constants and carrier lifetimes[71], realizing high-frequency responses of 3.6 GHz and 1.4 GHz for blue and green devices, respectively, as shown in Fig. 4(a). Regarding structural innovation, in Fig. 4(b–c), Xu et al. leveraged V-pits and sidewall quantum wells to create dual injection channels, significantly enhancing radiative recombination[72]. A multi-color array based on this structure achieved a total rate of 31.38 Gbps. Furthermore, Pezeshki et al. demonstrated an ultra-large-scale integration scheme by flip-chip bonding a 304-channel Micro-LED array with complementary metal oxide semiconductor (CMOS) driver circuitry[10]. This system attained a total capacity of 1 Tbps with a per-channel rate of 3.3 Gbps, highlighting the immense potential of massive parallel optical interconnects.

LDs operate based on the principle of stimulated emission, possessing significantly higher modulation bandwidths and superior spectral purity. Research on LDs-VLC

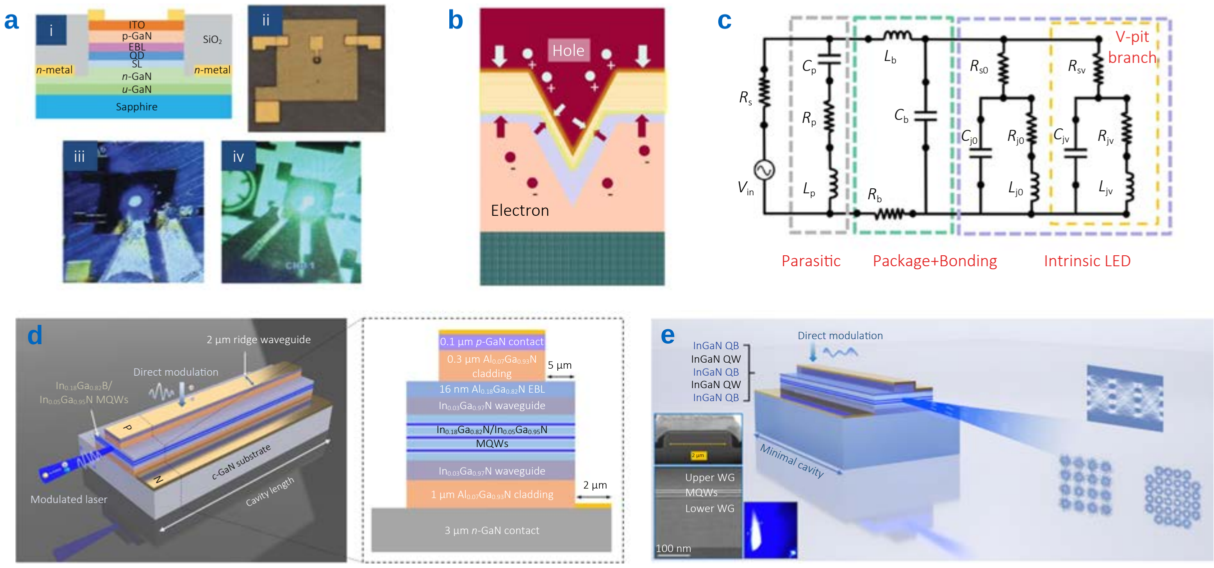

Fig. 4 | Schematic diagrams of various visible light transmitters structure. (a) Structure of the InGaN micro-LEDs. (b, c) The vertical profile of the V-pit structure and the proposed equivalent circuit for fitting both LEDs with and without V-pits. (d) 3-D structure of the laser chip and the layered epitaxial material structure. (e) 3D schematic diagram of a directly modulated GaN-based laser. Figure reproduced with permission from: (a) ref.[71], IEEE; (b, c) ref.[72], under a Creative Commons license; (d) ref.[44], Elsevier; (e) ref.[73], John Wiley and Sons.

systems focuses on resonant cavity design, micro-fabrication processes, and bandgap engineering. Based on rate equation theory, Li et al. shortened the cavity length and reduced the waveguide layer thickness to fabricate blue and green LDs with bandwidths of 5.4 GHz and 3.5 GHz[74], respectively. Wang et al. further miniaturized the device into a mini-LD with a ridge width of only 1.8 μm and a cavity length of 500 μm[41], achieving a 5.9 GHz bandwidth and 20 Gbps transmission. They also established a comprehensive carrier-photon dynamic model, predicting that an ultra-short cavity of 200 μm (Fig. 4(d)) could yield bandwidths exceeding 10 GHz[44]. In material band engineering, Jia et al. innovatively replaced traditional GaN barriers with InGaN quantum barriers to suppress the quantum confined stark effect (QCSE) as shown in Fig. 4(e)[73], boosting the bandwidth beyond 8 GHz and setting a record single-channel blue light communication rate of 36.5 Gbps. Additionally, utilizing multi-dimensional multiplexing technologies, Hu et al. and Lu et al. achieved ultra-high-speed transmissions of 46.4 Gbps (via red, green and blue (RGB) integration) and 170.1 Gbps (via 5-wavelength wavelength and polarization division multiplexing)[35,51], respectively, thereby significantly expanding the capacity of VLC systems.

2.2 Receiver and array photodetectors

In visible-light receivers, device platforms are still predominantly silicon-based. To mitigate silicon's limited responsivity in the short-wavelength visible band, ultraviolet (UV)-enhanced Si materials may be used. However, photodiodes (PDs) dedicated to short-wavelength operation have long been relatively underexplored. Detectors targeting short wavelengths typically employ wider-bandgap materials and are therefore less susceptible than Si-based detectors to interference from longer-wavelength optical signals or high-energy radiation.

In 2023, Xu et al. reported a series of Si-substrate GaN-based photodetectors with different superlattice interlayer period numbers in Fig. 5(a)[75], showing that increasing the superlattice periods improves the achievable rate: mini-PD samples with 8/15/32 periods reached 6.6/7.3/8.8 Gbps, while a micro-PD achieved 14.38 Gbps without waveform-level post-equalization and 15.26 Gbps with an neural network (NN)-based post-equalizer. In 2024, Xu et al. demonstrated a Si-substrate GaN/InGaN multi-quantum well (MQW) micro-PD array incorporating a V-pit structure within the MQWs in Fig. 5(b) to facilitate carrier transport and extraction under reverse bias, achieving a net data rate exceeding 12 Gbps[76].

Under low-light conditions, PDs without internal gain generate relatively few photoelectrons and are thus more susceptible to the thermal noise of subsequent amplification stages[77], leading to a lower signal-to-noise ratio than avalanche photodiodes (APDs) and photomultiplier tubes (PMTs). APDs and PMTs provide internal gain and higher responsivity. Consequently, under low-light conditions they are less affected by the thermal noise of subsequent amplification stages and can achieve a higher signal-to-noise ratio. In 2021, Milovancev et al. demonstrated a fully integrated 800 μm diameter Si APD optical receiver fabricated in a standard 0.35 μm BiCMOS process[78], achieving a sensitivity

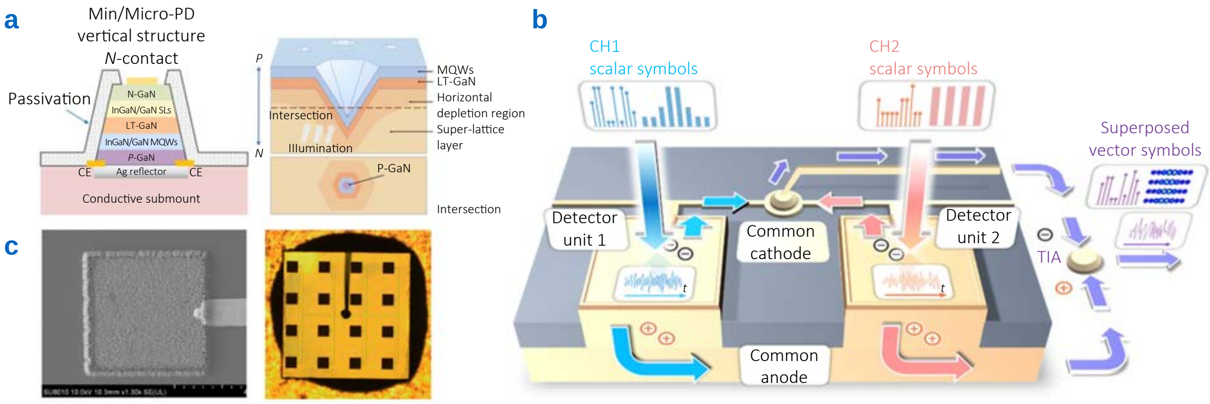

Fig. 5 | Schematics of representative visible-light receiver devices. (a) Vertical device architecture of the mini-PD and micro-PD, highlighting the V-pit structure and the superlattice pre-layer; the horizontal depletion region is indicated in the cross-sectional view. (b) Three-dimensional schematic of the detector array and signal superposition through the shared cathode/anode interconnection. (c) Vertical cross-section of the Si-substrate micro-LED-based photodetector and top-view layout of the 4 × 4 Si-substrate micro-LED array; scanning electron microscope (SEM) images and optical micrographs of arrays with 10, 50, and 100 µm chips. Figure reproduced with permission from: (a) ref.[75], Optica Publishing Group; (b) ref.[76], Chinese Laser Press; (c) ref.[85], Chinese Laser Press.

of −33 dBm at 1 Gbps and error-free VLC transmission distances up to 27 m. In 2022, Fei et al. employed a wideband PMT receiver for underwater wireless optical communication (UWOC), achieving a 100.6 m link and a 3 Gbps data rate, with a receiver sensitivity as low as −40 dBm for a 1.5 Gbps on-off keying (OOK) signal[79]. In 2025, Chen et al.employed a PMT-based ultraviolet communication receiver operating in a detectable-pulse mode and showed that, with adaptive threshold updating for pulse decision, the frame error rate (FER) was reduced from 0.303 to 0 at 10.4 m and from 0.95 to 0 at 5.6 m; under background variations emulating sunlight changes, the FER decreased from ~0.18 to 0 after threshold convergence[80].

Recently, single-photon detector (SPD)-based experiments have also been reported. Owing to their excellent sensitivity, SPD-based underwater systems are expected to support link distances beyond 100 m with data rates up to 1 Mbps[81]. Huang et al. emulated water-channel attenuation in the laboratory using optical attenuators, corresponding to an equivalent transmission distance exceeding 500 m[82]. At a received optical power of −84.3 dBm, they achieved 6.21 Mbps with a bit error rate (BER) of 1×10^{-7}, requiring on average only 1.35 photons per bit.

In VLC systems, the receiver's field of view (FOV) significantly influences both link stability and coverage. Conventional planar photodetectors typically exhibit narrow effective acceptance angles, causing rapid performance degradation under angular misalignment or slight movements between the transmitter and receiver. To address this limitation, efforts have focused on two main directions: optical hardware design and material innovation. Early approaches primarily relied on optical components such as concentrators[83] and intelligent reflecting surfaces[84] to expand the receiver's FOV. Array architectures can also be used to enlarge the effective receiving area of receivers. In 2022, Shi et al. employed a self-designed LED-based micro-PD array, as shown in Fig. 5(c), and experimentally achieved 10.14 Gbps over a 1 m free-space VLC link[85]. In 2025, Xu et al. demonstrated an integrated, parallel-connected 4 × 4 detector array to enhance light collection for wide-coverage reception. They achieved 12 Gbps for the dedicated communication channel and 200 Mbps for the broadcast channel, and reported a maximum broadcast field of view of 132.8°[86]. More recently, researchers have explored novel materials with intrinsic wide-angle characteristics[87]. To further enhance the effective reception range, fluorescent fiber-based photodetector architectures have been proposed, in which fluorescent materials absorb incident light at large angles and re-emit it toward the detector, achieving a balance between wide FOV and high sensitivity[88]. In 2025, Lin et al. demonstrated a $CsPbBr_3$ quantum-dot-based fluorescent antenna capable of supporting a communication rate of 1.23 Gbps with an FOV of ±60°[89]. Such advances provide VLC systems with improved adaptability and robustness.

Overall, recent advances in transmitter and receiver devices have significantly expanded the achievable bandwidth, power, and sensitivity of VLC systems. In practical implementations, device selection should be tailored to link distance, system mobility, and ambient-light conditions. Continued progress toward higher bandwidth, higher optical power, and higher sensitivity is expected to provide a solid hardware foundation for next-generation high-speed VLC networks.

3 Signal processing algorithm

Visible light communication systems are typically based on intensity modulation and direct detection, which inherently suffer from device noise, bandwidth limitations, nonlinear distortions, and channel impairments. To improve reliability and spectral efficiency under these constraints, advanced signal processing algorithms are essential, covering coding and modulation, channel estimation, and equalization techniques.

3.1 Coding and modulation

In VLC, the IMDD constraint requires the transmitted waveform to be real-valued and unipolar, and practical VLC transmitters usually do not have optical in-phase and quadrature (IQ) modulators. Under these constraints, carrier-less amplitude and phase (CAP) modulation is widely used for high-speed VLC. In Fig. 6(a), CAP applies constellation mapping to coded bits and then shapes the in-phase (I) and quadrature (Q) symbol streams with a pair of orthogonal pulse-shaping filters, typically formed by multiplying a square root raised-cosine (SRRC) pulse with cosine/sine functions. This process performs modulation and frequency translation and generates a real-valued single-subband CAP signal. The roll-off factor is an important parameter because it determines the occupied bandwidth and the samples per symbol.

For high-order CAP, Chi et al. combined hardware pre-equalization with a three-stage hybrid post-equalizer[90]. To

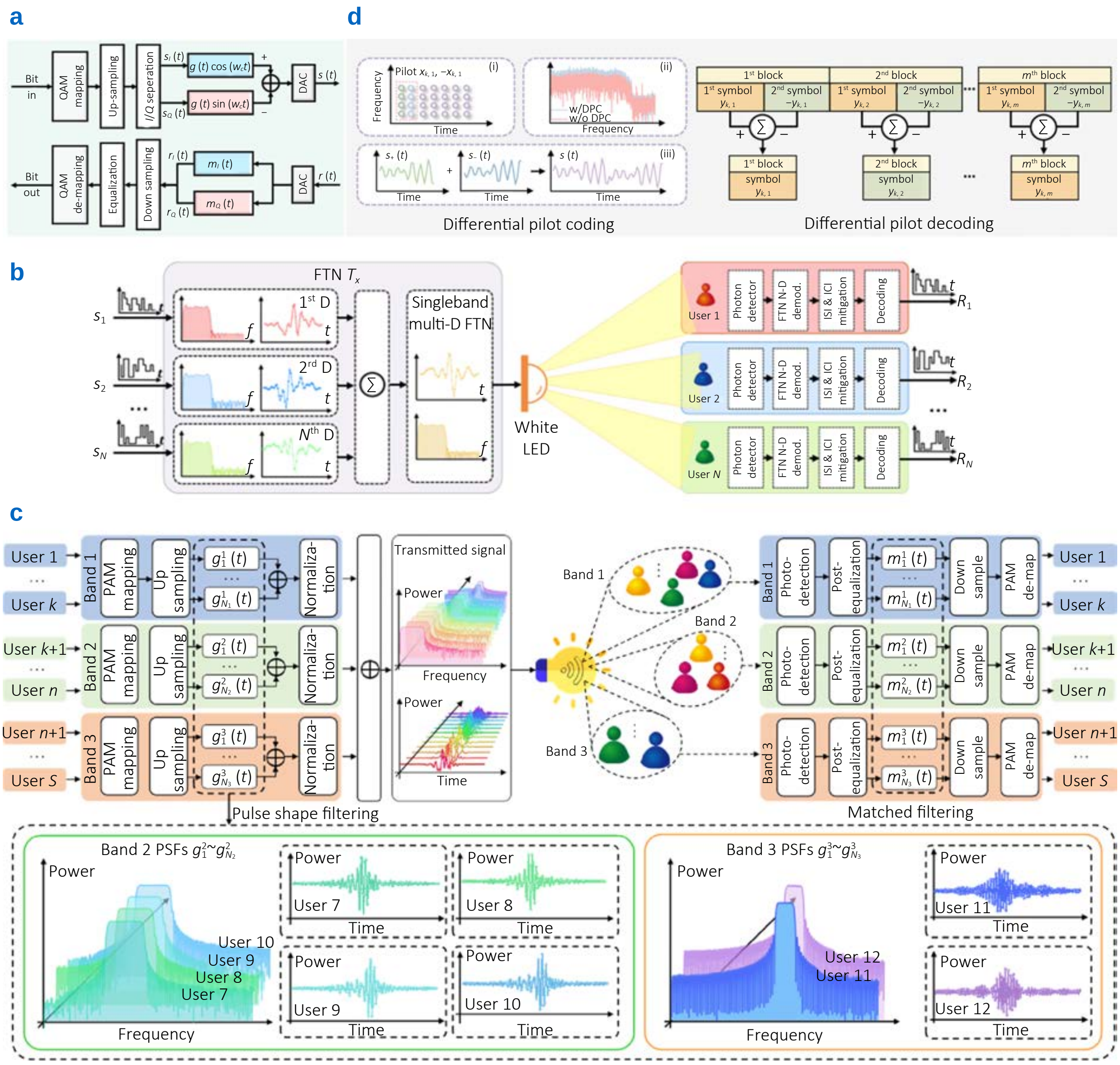

Fig. 6 | Advanced modulation and coding schemes for high-speed VLC. (a) Principle of CAP modulation and de-modulation. (b) Single band multi-dimension FTN scheme. (c) Flexible multiband N-dimensional CAP framework for configurable multiuser access. (d) DPC concept for VLC. Figure reproduced with permission from: (b) ref.[92], IEEE; (c) ref.[94], Optica Publishing Group; (d) ref.[16], Chinese Laser Press.

improve spectral efficiency and support multiuser access, non-orthogonal multiband CAP has been investigated. The mapped data are split into several subbands for different users, and each subband is generated by pulse shaping, without FFT/IFFT. Wang et al. introduced a spectral compression factor to reduce the sub-band spacing and compress the occupied bandwidth, which increases inter-subband interference and thus requires interference cancellation[91]. In Fig. 6(b), Lin et al. proposed N-dimensional CAP, where multiple users share the same band without guard bands. But this design brings intersymbol interference (ISI), and they used a slicing sphere decoder to detect symbols with moderate complexity[92]. Experimentally, a maximum bandwidth compression ratio of 70% was reported at a BER threshold of 3.8×10^{-3}, yielding a 42.9% spectral-efficiency gain over orthogonal CAP. For suppressing ISI in N-dimensional CAP systems, Nie et al. proposed a gapped index modulation scheme[93]. By applying structured, intermittent index modulation at the transmitter, the receiver can more effectively distinguish and recover signals affected by crosstalk. This approach enhances crosstalk resilience while maintaining relatively low complexity, allowing the use of smaller compression factors (i.e., narrower bandwidths) to achieve the same target data rates compared with conventional methods[93]. In Fig. 6(c), Lin et al. further extended this idea to multiband N-dimensional CAP[94], using frequency-division multiplexing across subbands and code-division multiplexing within each subband, enabling flexible configurations of subbands, users, and rates.

Besides CAP-based schemes, in direct-current biased optical orthogonal frequency division multiplexing (DCO-OFDM) with bit loading, the integer-bit constraint per subcarrier can limit the rate. Zhang et al. used pairwise coding across subcarrier pairs to balance the symbol error rate (SER) and achieved about 12%–33% rate improvement at medium-to-high SNR[95]. In Fig. 6(d), Zhou et al. proposed differential pilot coding (DPC) to suppress the direct current (DC) component and signal-signal beat interference (SSBI) in pilot processing[16], improving channel estimation and linear impairment compensation. In a 50-wavelength wavelength division multiplexing (WDM) VLC system, they demonstrated a 601.46 Gbps signal transmission.

3.2 Channel estimation

Channel estimation in VLC is fundamentally complicated by the coexistence of statistical channel randomness, such as scattering and turbulence induced fading with temporal variations, hardware-induced linear and nonlinear distortions caused by bandwidth limitation and optoelectronic nonlinearity, and non-ideal noise that is often signal dependent. In the model-driven paradigm, the received signal is characterized by an explicit parametric model and the channel is inferred using estimators such as maximum likelihood (ML), maximum a posteriori probability (MAP), least square (LS) and minimum mean square error (MMSE). Yaseen et al. established a representative benchmark by jointly considering a statistical random channel gain and input signal-dependent shot noise, deriving the Bayesian Cramér-Rao lower bound, and discussing practical estimation when the shot-noise factor is unknown at the receiver, which provides a rigorous reference for assessing learning-based designs under realistic noise conditions[96]. Nevertheless, when composite underwater or free-space impairments and non-Gaussian disturbances dominate, model mismatch becomes increasingly pronounced, and the pilot overhead and computational cost can rapidly increase in higher-dimensional settings.

Motivated by these limitations, a series of learning-based channel estimation methods have been proposed to either learn the mapping from pilots to channel state information or recast channel recovery as structured denoising. In 2020, Wu et al. proposed a deep neural network based channel estimation scheme for DCO-OFDM VLC that learns the nonlinear mapping from pilot observations to channel responses, enabling pilot reduction while maintaining competitive detection performance[97]. In the same year, Gao et al. introduced an FFDNet-based estimator for massive MIMO VLC by treating the channel matrix as a structured two-dimensional object and leveraging a fast and flexible denoising convolutional network to improve estimation accuracy over classical MMSE baselines[98]. In 2023, Rahman et al. proposed ResCBDNet, which incorporates noise-level estimation and residual blind denoising to enhance generalization to practical noise conditions beyond simplified Gaussian assumptions, thereby improving indoor massive MIMO VLC channel prediction across a wide SNR range[99]. For UVLC, Liu et al. proposed a block-sparse learning enabled channel estimation framework that unfolds an approximate message passing procedure into a deep-unfolding network and introduces a Gaussian-mixture denoiser to better exploit the block-sparse channel structure, particularly under low SNR or insufficient pilots[100]. Cai et al. further proposed a physical-prior-inspired ensemble learning approach that decomposes the UVLC channel into components associated with ISI-related linear distortion, SSBI-related quadratic distortion, and higher-order device distortion, and then learns them using a three-subnetwork ensemble, improving fidelity compared with both least mean squares (LMS) and single-network estimators[101].

Beyond direct channel state information (CSI) estimation, recent studies increasingly emphasize learning a realistic and differentiable channel model and integrating it into task-driven end-to-end optimization, as illustrated by Fig. 7(a–c). Wei et al. proposed an optical wireless channel simulator that jointly learns deterministic distortion and random noise, enabling more realistic channel modeling than approaches that only capture deterministic effects, and thus supporting digital-twin-style system analysis and optimization, corresponding to Fig. 7(a)[102]. Jin et al. proposed a two-

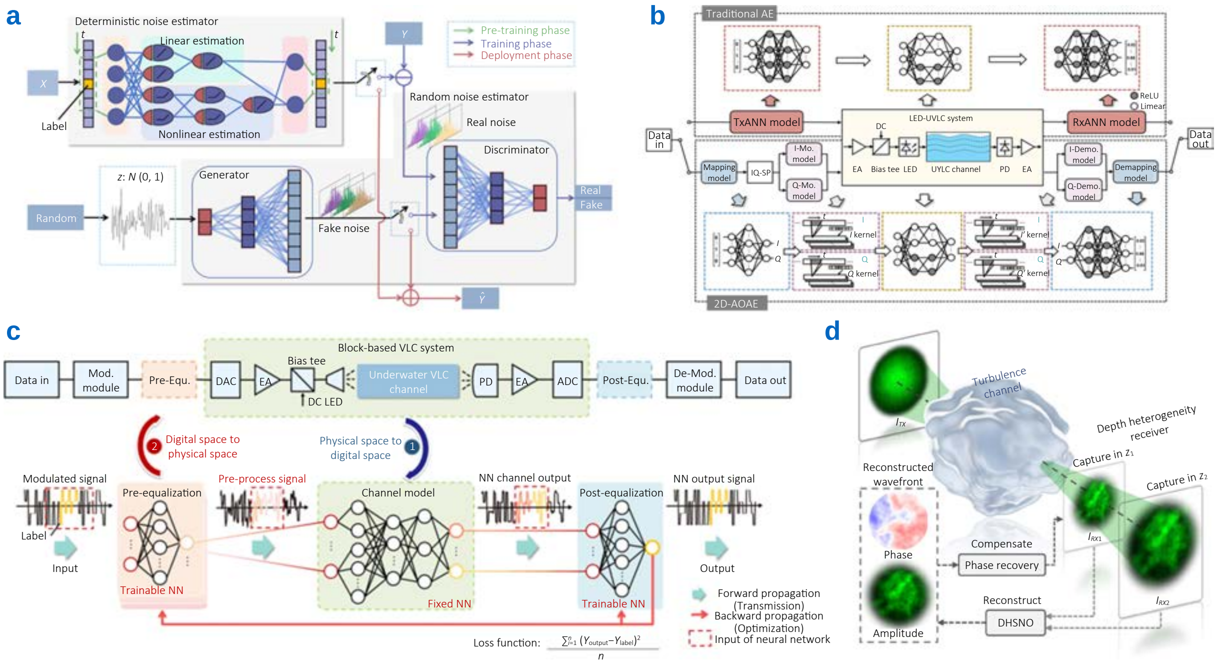

Fig. 7 | Representative learning-based frameworks for channel estimation/modeling and spatial-domain enhancement in VLC. (a) Deterministic-random noise joint channel simulator. (b) Autoencoder-style end-to-end transceiver optimization. (c) NN-based channel modeling with trainable pre-/post-equalization. (d) DHSNO-enabled single-pass wavefront reconstruction for turbulence correction. Figure reproduced with permission from: (a) ref.[102], IEEE; (b) ref.[103], Optica Publishing Group; (c) ref.[104], IEEE; (d) ref.[106], John Wiley and Sons.

dimensional adaptive optimization autoencoder that jointly optimizes signal generation and reception in underwater VLC (UVLC), emphasizing task performance rather than explicit CSI fidelity, corresponding to Fig. 7(b)[103]. In parallel, Shi et al. proposed a neural network-based auto equalization model for UVLC that consists of a neural channel model together with pre-equalization and post-equalization networks trained in an end-to-end manner, enabling adaptive pre-equalization under bandwidth-limited and nonlinear link conditions, corresponding to Fig. 7(c)[104]. Complementarily, Chen and Jiang proposed a blind detection network that jointly addresses blind channel estimation, equalization, and data detection by learning inverse-channel features directly from received signals, providing an alternative route to integrate estimation and detection when pilots are scarce or unavailable[105].

Spatial-domain information provides another important avenue to reduce overhead and improve robustness, particularly for high-dimensional cascaded channels and turbulence-dominated links. Sun et al. proposed a joint space-time sampling protocol for optical intelligent reflecting surface assisted VLC that exploits spatial and temporal coherence to reduce pilot overhead and enable scalable CSI acquisition under an alignment-based cascaded channel model[107]. Zhang et al. proposed a depth heterogeneity self-supervised neural operator that leverages a depth-heterogeneity receiver and embeds propagation physics as fixed forward operators, enabling single-pass wavefront reconstruction and turbulence correction without requiring labeled wavefront data, corresponding to Fig. 7(d)[106]. Overall, these representative works indicate that channel estimation for VLC/UVLC is evolving from purely analytical estimators toward hybrid physics-and-learning solutions and end-to-end optimization, with realistic channel modeling and spatial-domain processing increasingly serving as key enablers for robust and scalable systems.

3.3 Pre-equalization technology

Pre-equalization is primarily introduced to compensate for high-frequency fading in visible light communication links. By boosting the high-frequency components of the transmitted signal, pre-equalization flattens the effective received spectrum, as illustrated in Fig. 8(a). In terms of implementation, pre-equalization can be broadly categorized into hardware-based and software-based approaches. Hardware pre-equalization typically relies on analog networks composed of resistors, capacitors, and inductors to reshape the frequency response. Fujimoto et al. incorporated a single-stage pre-equalization branch into an LED driver[108], using a bypass path to provide high-frequency enhancement of the modulation signal. However, it should be noted that a single-stage network generally offers limited compensation depth. To further extend the effective bandwidth, Huang et al. proposed a two-stage cascaded constant-resistance bridged-T amplitude equalizer (see Fig. 8(b) for the topology and

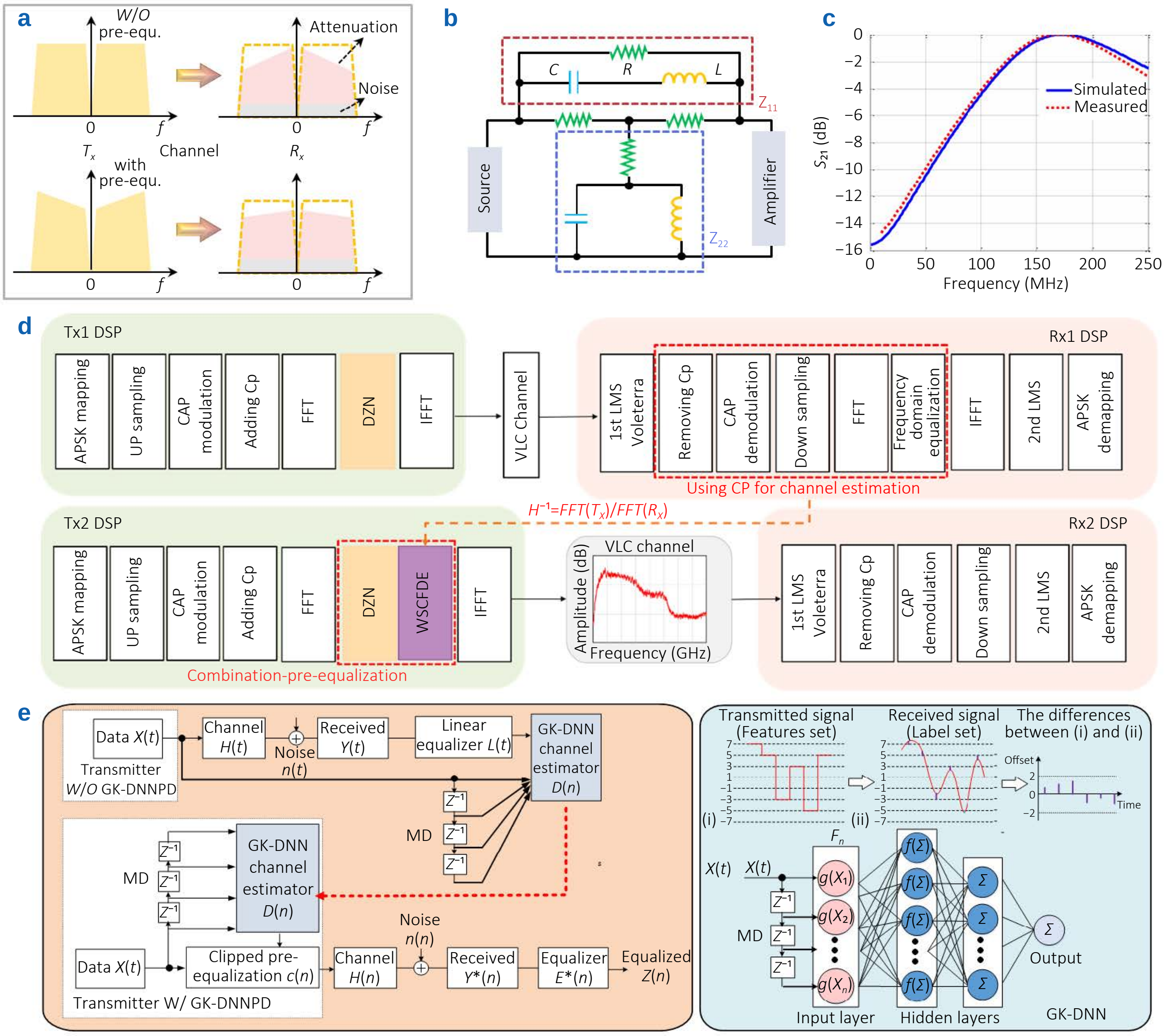

Fig. 8 | Schematic illustration of pre-equalization techniques. (a) Conceptual principle of pre-equalization. (b) Hardware pre-equalizer circuit and (c) corresponding frequency response: the two-stage cascaded constant-resistance bridged-T amplitude equalize. (d) Software-based pre-equalization algorithm: Windowed single-carrier frequency-domain pre-equalization (WSCFDE). (e) AI-assisted software pre-equalization algorithm: Gaussian-kernel-aided deep neural network (GK-DNN). Figure reproduced with permission from: (c) ref.[110], IEEE; (d) ref.[111], IEEE.

Fig. 8(c) for the response)[109–110]. The equalizer introduces moderate attenuation at low frequencies while providing stronger compensation in the mid-to-high frequency range, thereby improving the utilization of the high-frequency band. Despite the bandwidth-extension capability, hardware equalizers are often constrained by impedance mismatch and limited configurability, which can be unfavorable for high-speed VLC signal transmission.

To overcome the limited tunability of hardware solutions, software-based pre-equalization has been widely studied to support response-aware adaptation and iterative refinement in practical channels. Chen et al. proposed a time-domain pre-equalization scheme based on the LMS adaptive algorithm in conjunction with a Volterra nonlinear filter[112], and further exploited transmitter-receiver cooperation by combining pre-equalization with receiver-side post-equalization to enhance overall robustness.

Zhang et al. developed a frequency-domain pre-equalization method based on the forward transmission coefficient (*S*-parameters)[113], which pre-compensates the channel low-pass attenuation using the inverse channel response. Khawatmi et al. proposed a real-time zero-forcing (ZF) pre-equalization strategy that smooths the inverse response with a short window and enforces an amplitude floor before frequency-domain ZF processing[114]. This design reduces noise enhancement while substantially extending the usable bandwidth, increasing the LED bandwidth from 8.3 MHz to 100 MHz. As shown in Fig. 8(d), Zhang et al. further proposed windowed single-carrier frequency-domain pre-equalization (WSCFDE)[111], which performs band selection and smoothing on the inverse response and applies pre-compensation only to the most significant sub-bands. Compared with full-band inverse filtering or simple power reallocation, WSCFDE offers improved robustness under a BER constraint, enabling 14 Gbps signal transmission over a 1 m free-space link. With the growing adoption of artificial intelligence (AI) in signal processing, AI-enabled pre-equalizers have increasingly emerged. As illustrated in Fig. 8(e), Zhao et al. employed a Gaussian-kernel-aided deep neural network (GK-DNN) for nonlinear pre-distortion in VLC[115], achieving a 1.56 dB *Q*-factor improvement with reduced training overhead, which indicates strong potential for modeling complex nonlinearities and integration into adaptive frameworks. In addition, Niu et al. proposed a neural-network-based Tomlinson-Harashima precoding scheme (NN-THP) as a digital pre-equalizer[42], simultaneously mitigating inter-symbol interference and system nonlinearity at the transmitter, and enabling WDM VLC with an aggregated throughput of 534.51 Gbps.

Pre-equalization improves the utilization of mid-to-high frequency components by pre-shaping the transmit spectrum and reallocating power, thereby improving the BER performance of VLC links. For high-speed VLC employing high-order modulation, it is expected to evolve from standalone frequency-response shaping to a joint transmitter–receiver optimization framework integrated with receiver-side post-equalization, enabling the simultaneous mitigation of linear distortion and nonlinear impairments. Meanwhile, AI is driving a shift from conventional inverse filtering and rule-based constraints toward online adaptation and data-driven approaches, offering a promising path to further gains under complex channels and real-time implementation constraints.

3.4 Post-equalization algorithm

Post-equalization is a receiver-side digital signal processing (DSP) procedure that mitigates residual impairments after optical-to-electrical conversion, including bandwidth-limited inter-symbol interference, optoelectronic nonlinearity, and in free-space or underwater links, turbulence-induced waveform fluctuations. Zhou et al. compared post-equalizers based on Volterra series model[116], memory polynomial model, memoryless polynomial model, and deep neural network (DNN) in a high-speed VLC system as shown in Fig. 9(a), and also analyzed how to select the most appropriate nonlinear equalizer under different conditions. As baud rate and modulation complexity continue to increase, conventional linear and Volterra-type equalizers often exhibit an unfavorable performance-complexity balance, which has stimulated extensive research on learning-assisted post-equalizers that improve robustness while keeping the implementation tractable.

A typical strategy is to embed a clear physical prior into a lightweight network structure. In 2020, Hu et al. proposed a low-complexity memory-polynomial-aided neural network post-equalizer, where a memory-polynomial expansion is used to explicitly represent nonlinear distortions with memory and a compact neural network then learns the residual mapping, as illustrated in Fig. 9(b)[117]. By combining structured nonlinear bases with a small trainable network, this approach achieves effective nonlinear compensation with reduced model size compared with a fully connected neural equalizer, and demonstrates clear performance gains over conventional post-equalization baselines in CAP-VLC experiments. An alternative route is to improve learning efficiency by transforming the received waveform into a feature domain that is more amenable to neural inference. Lu proposed a discrete-wavelet-transform assisted convolutional neural network (CNN) equalizer, which leverages multiresolution analysis to separate distortion components across scales before CNN-based compensation, and experimentally shows improved robustness compared with classical and neural baselines in VLC[118]. Compared to traditional algorithms like Volterra equalizers, network-assisted methods expand the operational range by approximately 29%. These approaches leverage physical-model-based compensation as a prior, with neural networks learning residual distortions, resulting in improved stability and generalization.

For longer-range visible-light laser communication, post-equalization must cope with stronger channel dynamics and nonlinearity while maintaining training efficiency. Lu et al. introduced a bidirectional reservoir computing equalizer for a 100 m visible-light laser link, where the reservoir provides a rich dynamic representation and only the readout layer is trained, significantly reducing training burden relative to dense neural models while achieving competitive performance at multi-gigabit rates[60]. When turbulence becomes dominant in underwater links, learning-based post-equalization increasingly relies on multi-dimensional observation and structured fusion. Lu et al. proposed a turbulence-resistant dual-aperture receiver with a sparse dual-polarization triple-branch network, where dual-polarization observations are processed in parallel branches and fused through sparse connections to enhance robustness[119]. Notably, when experimental conditions shift from pure water to varied turbidity, salinity, or bubble-induced disturbances, the network continues to function without retraining, sustaining transmission rates above 140 Gbps. Building on the same "diversity plus fusion" principle, Zhou et al. further combined single-transmitter multi-receiver diversity with a triple-branch neural waveform equalizer and an attention

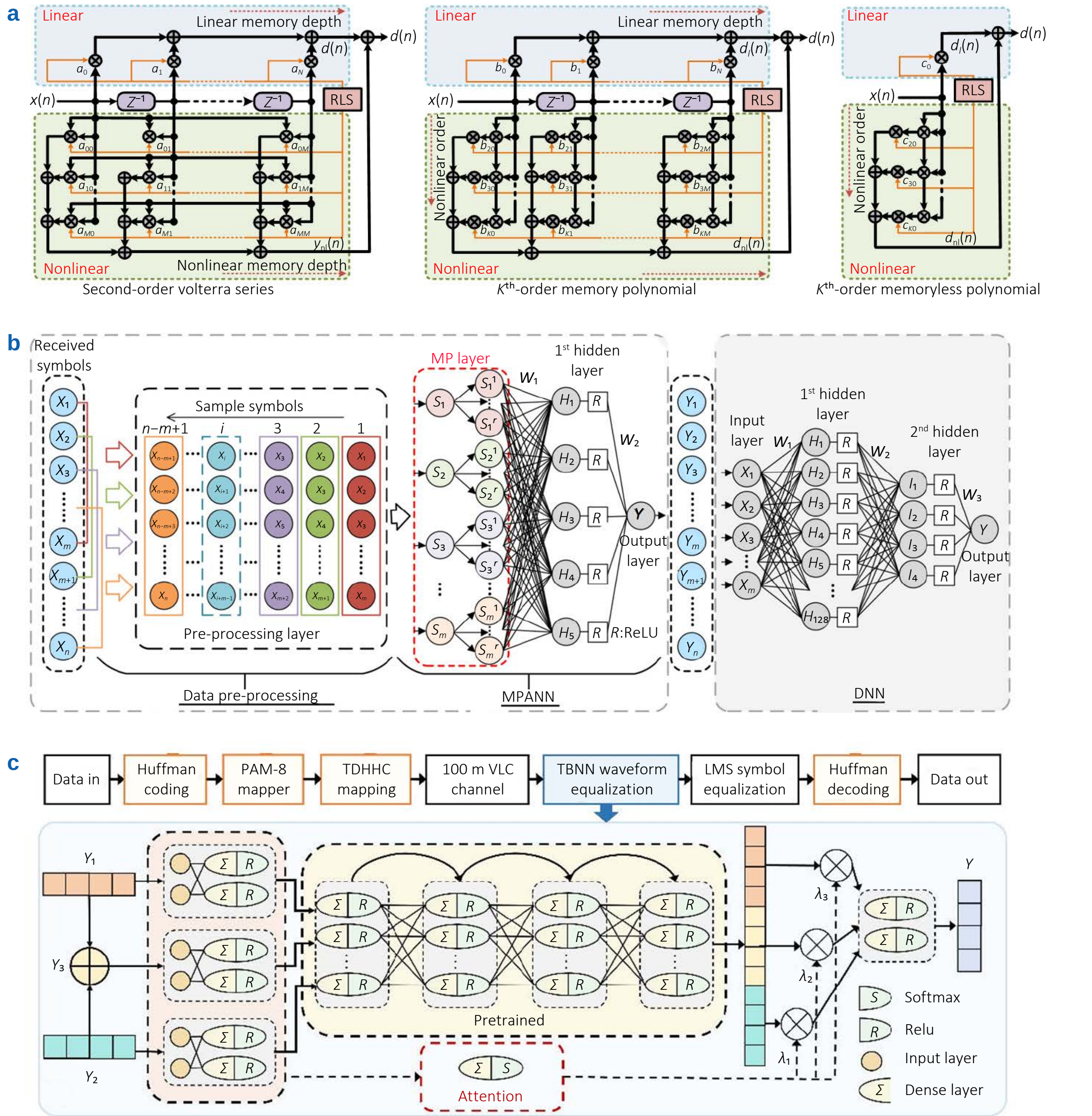

Fig. 9 | (a) Structures of the Volterra series model, memory polynomial model and memoryless polynomial model. (b) Principle of the low-complexity memory-polynomial-aided neural network post-equalizer. (c) A triple-branch waveform equalizer with attention mechanism. Figure reproduced with permission from: (a) ref.[116], Optica Publishing Group; (b) ref.[117], under a Creative Commons license; (c) ref.[61], Optica Publishing Group.

mechanism that adaptively weights branch features under varying channel states, as depicted in Fig. 9(c)[61]. These results indicate that post-equalization gains can be amplified when receiver diversity and network fusion are co-designed, particularly for turbulence-affected or long-range visible-light links.

The generalization capability of NN-based equalizers remains a critical performance metric. Beyond integrating physical priors, sparsification, and lightweight designs to mitigate overfitting, online adaptive fine-tuning can further enhance robustness. NN equalizers inherently learn the nonlinear mapping between distorted input waveforms and transmitted symbols. When the test channel deviates significantly from the training distribution (e.g., under sudden strong turbulence or rapid motion), performance may degrade. In such cases, online adaptive tuning or transfer learning can quickly adapt pre-trained models to new channel conditions. Compared with full retraining, these strategies substantially reduce computational cost while preserving high performance[120]. The above works show a clear progression from general neural equalization toward approaches that are increasingly structure-aware and implementation-oriented, including prior-assisted lightweight learning, transform-assisted feature learning, training-efficient reservoir computing, and diversity-aware multi-branch fusion with adaptive weighting. Future work should further address real-time latency, cross-condition generalization, and the joint design of training overhead and adaptation speed for rapidly varying channels.

4 System and network architecture

Conventional point-to-point VLC links face inherent limitations in achieving orders-of-magnitude increases in transmission capacity. In addition, single-dimensional signal observation provides only partial channel awareness, which restricts effective interference suppression and robustness enhancement. As a result, system architectures that exploit multi-dimensional multiplexing and multi-dimensional channel observation have emerged as essential enablers for next-generation high-capacity and high-reliability VLC networks.

4.1 Multi-aperture reception technology

In visible light communication systems, signals encounter interference from numerous complex environmental factors during propagation. These include light intensity scintillation, beam drift, and wavefront distortion caused by turbulent effects such as scattering and attenuation in seawater or atmospheric channels. Consequently, SNR degradation and signal distortion occur, making it highly challenging to achieve high-reliability signal transmission using simple P2P systems[121]. Considering that turbulence and noise affect optical signals differently across various dimensions or modes[122–123], this presents a novel optimization strategy for efficient, high-reliability information transmission: multi-aperture reception technology. This technique decomposes the same information into multiple high-dimensional components, including spatial, polarization, mode, and depth information. It fully leverages the independence of these optical channels during transmission. At the receiver end, multi-aperture technology extracts components from each dimension to obtain richer channel information, thereby enhancing signal reconstruction capabilities. Figure 10(a) illustrates a schematic of a multi-aperture reception system based on spatial and polarization decomposition.

Over the past two years, researchers have analyzed and validated the effectiveness of multi-aperture reception technology. Meanwhile, a series of explorations have been conducted on signal fusion and reconstruction algorithms for multi-aperture reception. In 2025, Hu et al. proposed a free-space visible light communication system based on polarization dual-aperture reception[124]. Circularly polarized light was transmitted, and the receiver collapsed the beam into horizontally and vertically polarized components for separate reception and subsequent merging. Using a humidifier to simulate atmospheric turbulence, the performance of polarization-based multi-aperture reception in mitigating turbulent interference was validated. Chen et al. applied this technique to an underwater visible light communication system[112], as shown in Fig. 10(b). Using WDM technology, they achieved a transmission rate of 39.54 Gbps in a 5 meter underwater channel. For this UVLC system, Feng et al. employed a wave-making pump to simulate underwater turbulence[125], as depicted in Fig. 10(c). They employed an adaptive symbol-level fusion algorithm with a weighted attention mechanism to merge and reconstruct the received signals. The fused signal exhibited a significantly reduced bit error rate compared to the original two separate signals, as shown in Fig. 10(d). Ultimately, a reliable data rate of 73.31 Gbps was achieved. Lu et al. proposed a multi-aperture receiving system combining spatial and polarization diversity. They reconstructed the received signals using a sparsely connected three-branch network, achieving stable transmission exceeding 140 Gbps under various turbulence intensities[119].

Multi-aperture reception technology not only effectively acquires richer channel information and optimizes signal processing workflows, but also enhances the interference resistance and overall transmission efficiency. By further focusing on deep learning-driven adaptive signal fusion and dynamic optimization, as well as the joint utilization of multi-dimensional information to enhance system redundancy and reliability, it is poised to become a key enabler for high-performance visible light communications.

4.2 Beamforming technology

Beamforming (BF) technology serves as a pivotal mechanism to circumvent the inherent line-of-sight (LOS) constraints and blockage sensitivity of VLC. By precisely orchestrating multi-dimensional light-field parameters to achieve directional energy focus, BF significantly bolsters the received SNR for ultra-high-speed transmission while mitigating multi-user interference via spatial isolation[126–128]. Its agile dynamic tracking further provides critical mobility robustness and underpins space-division multiple access (SDMA) efficiency, establishing BF as a cornerstone for high-performance optical wireless networks.

At the system level for multi-user access and resource management, beamforming is increasingly integrated with advanced multiple access schemes to maximize spectral efficiency. Liu et al. combined BF with non-orthogonal multiple access (NOMA) to facilitate multi-user multiplexing in

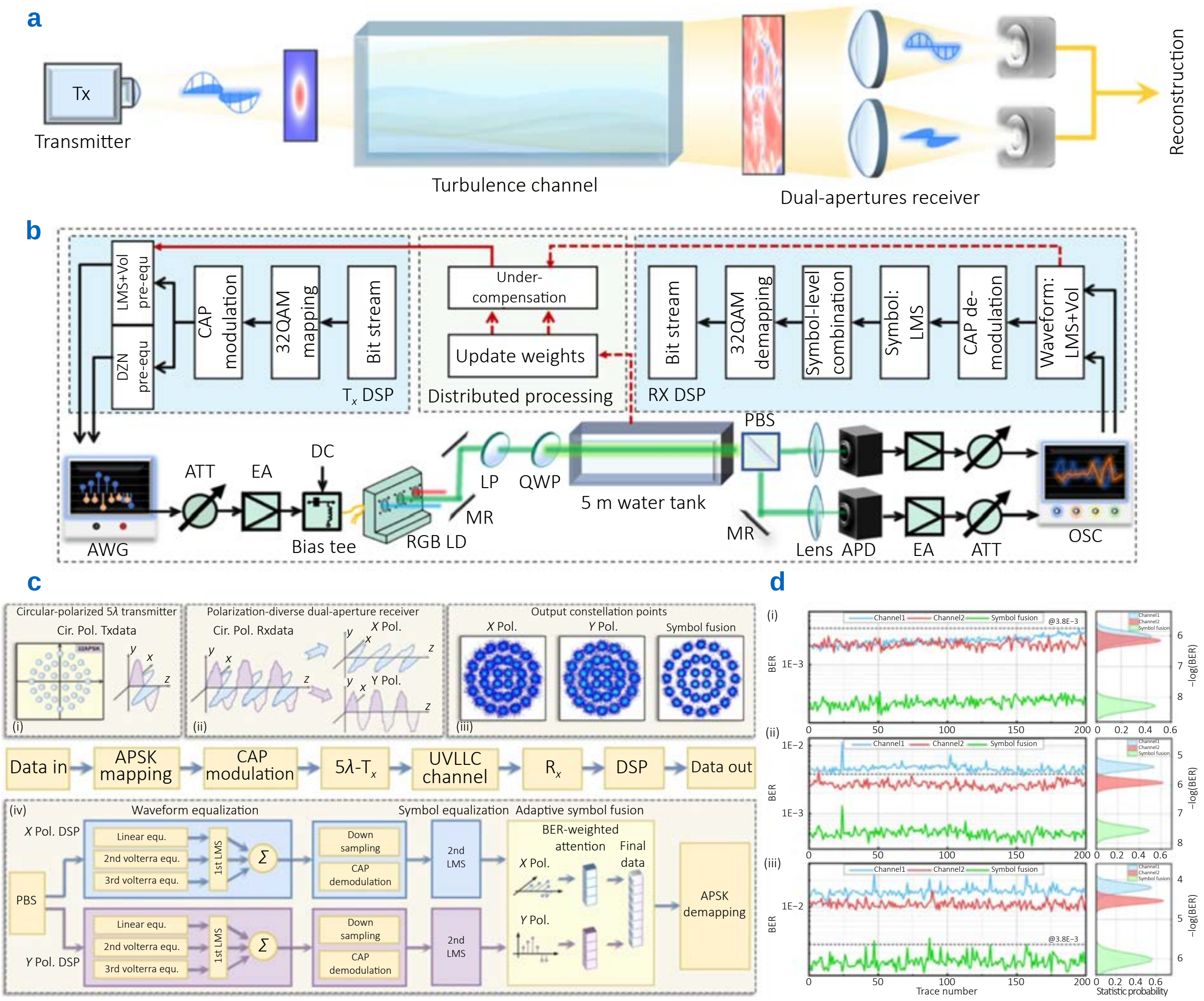

Fig. 10 | (a) Schematic diagram of a spatial and polarization diversity dual-aperture receiving system. (b) Underwater dual-polarization receiving system based on an RGB laser transmitter module. (c) Principle of the dual-polarization receiving system based on an adaptive symbol-level fusion algorithm. (d) BER fluctuation of the fused signal compared to the two original received signals. Figure reproduced with permission from: (b) ref.[112], IEEE; (c, d) ref.[125], Chinese Laser Press.

the power domain, as shown in Fig. 11(a)[129], significantly optimizing resource allocation and connection density in high-density scenarios. To support such complex spatial resource orchestration, VLC beamforming hardware is evolving from traditional macro-scale modulation toward chip-scale solid-state control, with thin-film lithium niobate (TFLN) and silicon-based integrated photonic platforms at the forefront of recent research. Studies by Ye et al. and Ma et al. have showcased the exceptional potential of TFLN-based optical phased arrays (OPA)[130,131], achieving single-channel transmission rates of 320 Gbps and multi-target two-dimensional steering by leveraging nanosecond-scale electro-optic responses and ultra-wide bandwidths as illustrated in Fig. 11(b). Furthermore, Lin et al. implemented independent multi-beam control via integrated acousto-optic arrays[135], while Wang et al. and Yue et al. respectively validated broadband silicon-based OPAs covering the full visible spectrum (RGB) and high-precision 2D pattern synthesis[132,136], signifying the maturation of all-solid-state chip-scale solutions in terms of throughput and reconfigurability.

Simultaneously, researchers have introduced intelligent reflecting surfaces and topological physical properties to enhance system robustness against signal attenuation and blockage. Sun et al. and Zhu et al. utilized optical intelligent reflecting surfaces (OIRS/RIS) to achieve autonomous beam reconfiguration and user localization[137,138], effectively improving coverage quality in non-line-of-sight (NLOS) paths. Niu et al. suppressed channel crosstalk through neural-network-aided wavelength multiplexing[133], as shown in Fig. 11(c), while the topological beamformer proposed by Wang et al. established a new design paradigm for high-gain wireless links[139]. For specialized high-bandwidth switching scenarios such as data center optical interconnects, as illustrated in Fig. 11(d), Li et al. achieved high-efficiency programmable optical switching using physical-model-inspired neural networks and spatial light modulators[134],

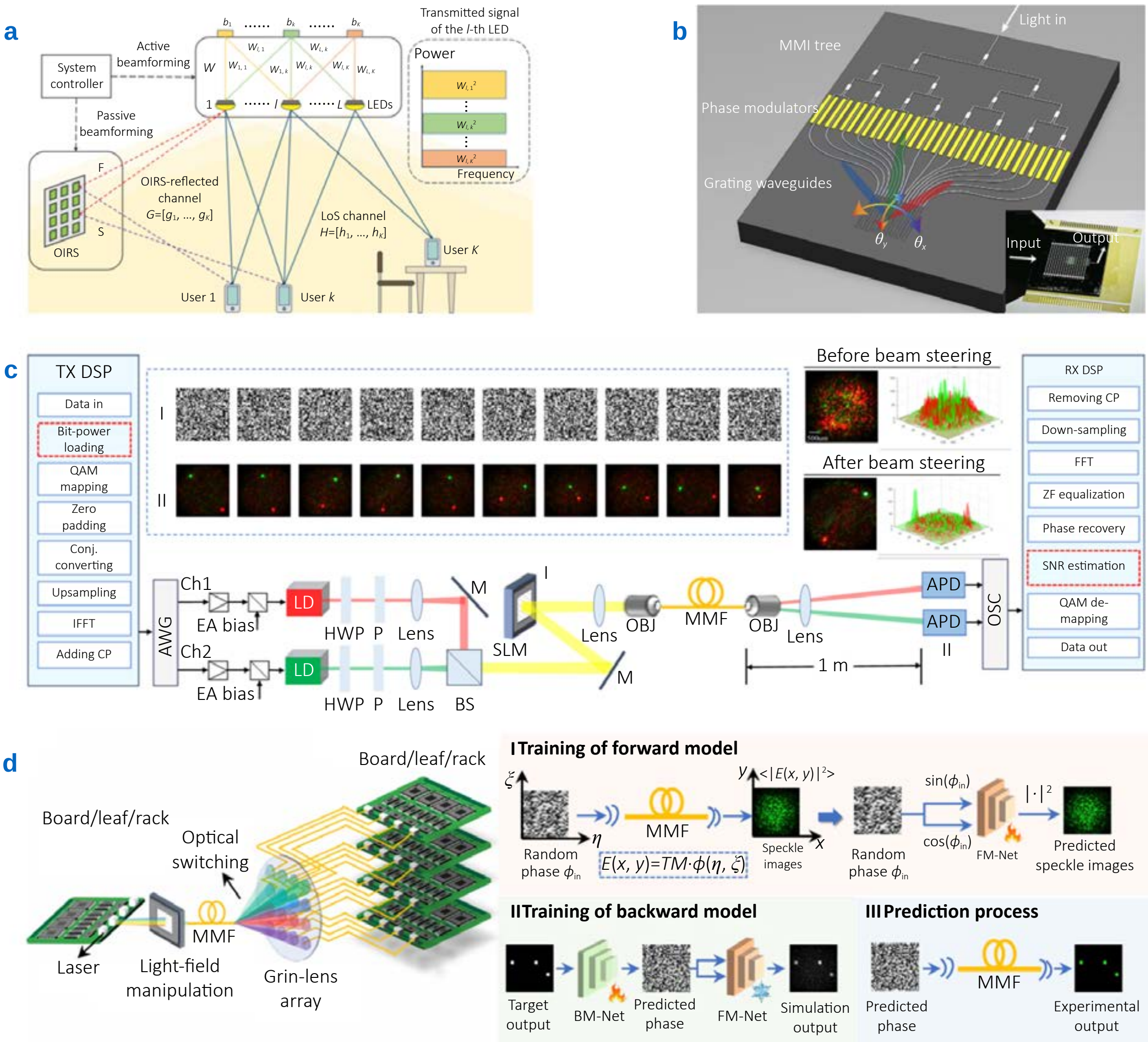

Fig. 11 | Several classical beamforming technical schemes. (a) System model of the NOMA-based MISO VLC with OIRS. (b) Integrated thin-film lithium niobate (TFLN)-based optical phased array. (c) Schematic diagram of a WDM-based hybrid fiber-VLC indoor access network. (d) Flexible and reconfigurable optical switching for data center interconnects. Figure reproduced with permission from: (a) ref.[129], IEEE; (b) ref.[132], Optica Publishing Group; (c) ref.[133], Optica Publishing Group; (d) ref.[134], Optica Publishing Group.

further optimizing communication performance in complex indoor environments through intelligent spatial propagation intervention. Looking ahead, beamforming technology will continue to advance toward larger-scale array integration to achieve narrower beamwidths and superior sidelobe suppression. Concurrently, the deep integration of artificial intelligence for real-time channel estimation and beam tracking, along with the exploration of multi-spectrum synergistic schemes, will remain the primary research directions.

4.3 Multi-dimensional multiplexing-based large-capacity VLC system

Signals in visible light communication can be multiplexed across multiple dimensions such as wavelength, polarization, spatial, and mode. For example, employing multi-antenna arrays at both the transmitter and receiver enables spatial multiplexing and diversity gain, offering a viable solution to overcome capacity limitations in visible light communication.

In underwater visible light communication systems, in 2022, Issaoui et al. achieved an 11 Gbps WDM VLC link by mixing RGB lasers through a thermally stable fluorescent plate and employing channel-adaptive direct current-biased optical orthogonal frequency division multiplexing[45]. In 2024, Hu et al. achieved a data rate of 20.1 Gbps over 100 meters in clean water using RGB WDM technology and a full-color meta-surface enabling Gaussian to Airy beam conversion[140]. In 2025, Lu et al. achieved transmission of 170 Gbps signals over a 1.2 m underwater link using a five-

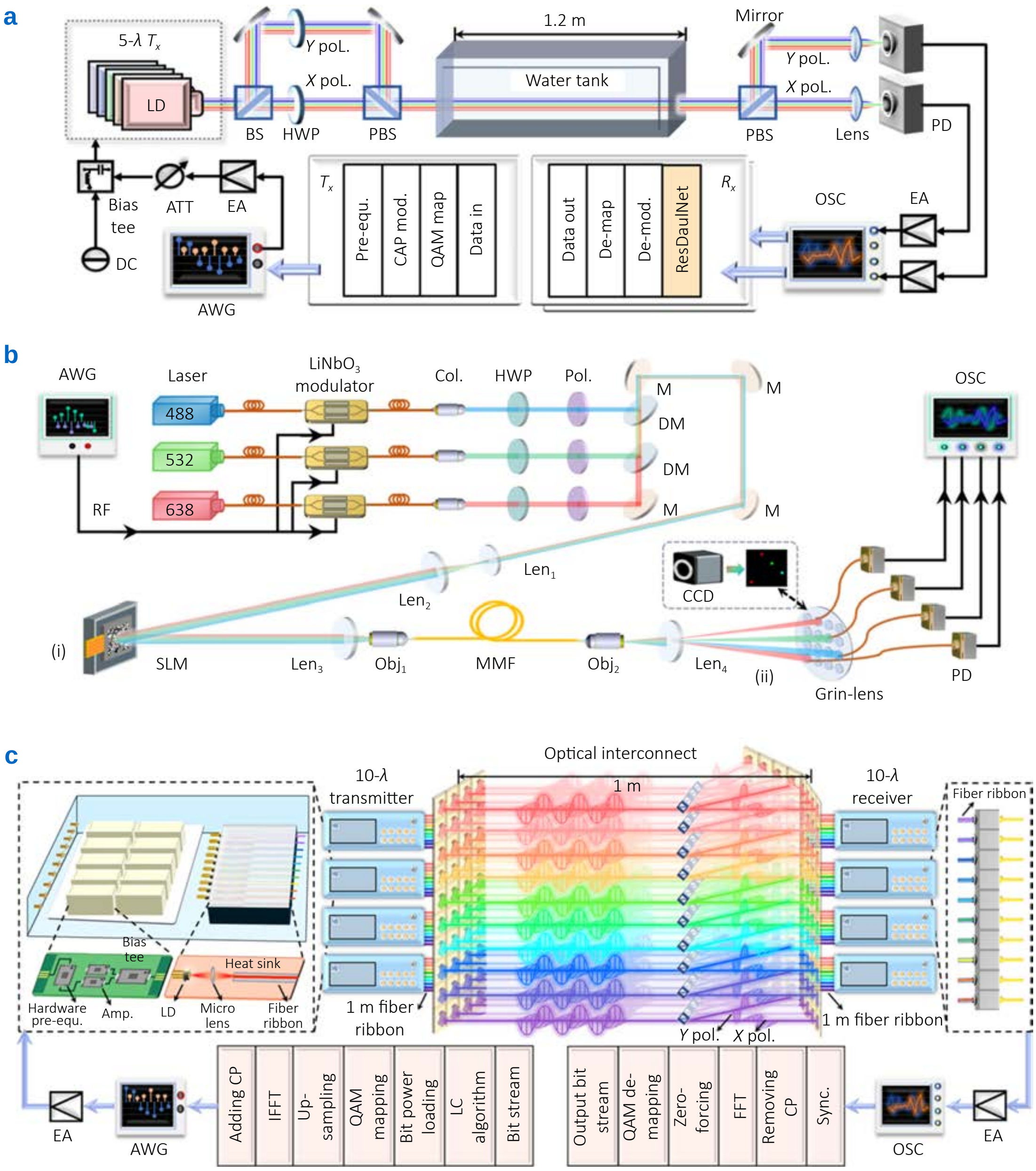

Fig. 12 | (a) A 170 Gbps underwater visible light communication system based on a five-wave laser transmission module. (b) Diagram of the VLLC experimental setup based on reconfigurable visible light optical switching system. (c) An 831 Gbps ultra-high-speed optical interconnect system based on a 40-λ visible light prototype transceiver. Figure reproduced with permission from: (a) ref.[51], Chinese Laser Press; (b) ref.[144], IEEE; (c) ref.[43], IEEE.

wavelength laser transmitter module and a post-equalization network with differential receiver[51], as shown in Fig.12(a).

MIMO technology leverages spatial parallelism to provide a cornerstone solution for surmounting bandwidth bottlenecks and enhancing resource scheduling flexibility in data center optical switching[141−143]. Recent research in spatial multidimensional interconnects emphasizes high-capacity transmission and agile link reconfigurability, with Li et al. employing a physics-inspired forward-backward network to enable programmable 1×16 WDM optical switching with a projected system throughput of 629.28 Gbps[144], as shown in Fig. 12(b). Concurrently, Wu et al. demonstrated a massive parallel optical link supporting 144 concurrent users with an aggregate capacity of 28 Tbps and a 120° wide field-of-view by utilizing meta-surface-integrated fiber arrays[145]. Furthermore, multidimensional interconnect technologies are increasingly advancing toward deeper on-chip integration, as seen in the work of Sun et al.[146], who achieved a record-breaking capacity of 38.2 Tbps across 88 wavelength channels using a packaged five-mode multiplexing chip. These advancements underscore that MIMO technology is poised for broader implementation within data center optical interconnects, continuously steering network architectures toward higher integration and multidimensional space-division multiplexing[147–148].

In multi-wavelength free-space visible light communication, in 2024, Lin et al. achieved a 519.21 Gbps fiber-free-space-fiber link transmission based on a 50-channel WDM system with discrete multi-tone (DMT) modulation[40]. In 2025, Zhou et al. achieved a 600 Gbps visible light communication system using this system with pilot differential coding technology[16]. Furthermore, Shi et al. achieved a breakthrough transmission rate of 805 Gbps and a spectral efficiency of 50.3 bit/s/Hz by integrating wavelength division multiplexing with orbital angular momentum (OAM) multiplexing[149]. Employing WDM combined with polarization division multiplexing, Lu et al. achieved an 831 Gbps communication rate over a 1 m free-space link using a 40-wavelength prototype transceiver[43], as shown in Fig. 12(c). This laid the foundation for Tbps-level VLC systems and further advanced VLC applications in data center interconnect scenarios.

By utilizing multiple dimensions of visible light beams, transmission rates can be significantly enhanced. However, multiplexing and de-multiplexing devices for visible light remain immature, making this a key research focus for future visible light communication. The maturity of multi-dimensional multiplexing devices is constrained by limitations in materials and fabrication technologies. For instance, high-speed, multi-wavelength, or multi-mode multiplexers typically require low-loss, highly uniform transparent optical materials and precise micro-structuring. Current silicon- or silicon-nitride-based platforms still face challenges in wavelength coverage, mode preservation, and crosstalk suppression[150]. Moreover, the performance of such devices is highly sensitive to the fabrication accuracy and uniformity of nanoscale waveguides and micro-gratings, which remains a key barrier to large-scale deployment[151,152]. Future research must achieve breakthroughs in material engineering, micro-fabrication processes, and integrated device design to enable high-performance visible-light multi-dimensional multiplexing. Although multiplexing technology can increase system capacity, it also substantially increases the complexity of system design and signal processing. Therefore, precise optimization and coordination of signal modulation and processing across multiple dimensions are required. Developing joint time-frequency-spatial multi-dimensional optimization techniques will further enhance the transmission efficiency and reliability of the system.

Beyond high-speed and high-capacity communications, visible light systems also offer the potential for integrated sensing and power delivery. Specifically, integrated sensing and communication (ISAC) based on visible light leverages the intrinsic properties of optical signals to enable environmental awareness[153], such as positioning or object detection, while simultaneously transmitting data. Additionally, visible light-based simultaneous lightwave information and power transfer (SLIPT) techniques allow low-power devices to harvest energy alongside information delivery, enhancing sustainability and efficiency in future networks[154]. Integrating these multifunctional capabilities into VLC system architectures highlights the potential for diversified deployment in next-generation 6G networks.

5 From laboratory prototypes to field-deployable VLC systems

With continuous advances in device performance, modulation schemes, and system architectures, VLC is gradually transitioning from laboratory demonstrations to real-world deployments. However, practical communication scenarios differ markedly from idealized experimental conditions. Factors such as strong ambient light, relative motion between transceivers, and complex, time-varying channel characteristics impose stringent requirements on system stability and reliability. Therefore, before large-scale application of VLC, it is essential to systematically review existing field trials and analyze the key engineering challenges and potential solutions for practical deployment.

In real-world VLC systems, strong background illumination like sunlight or ambient lighting introduces significant DC offsets and random noise, compressing the receiver's dynamic range and degrading SNR, which critically affects link stability. Early studies addressed this issue using narrowband optical filters combined with high-pass circuits to suppress broadband sunlight[155], laying the foundation for outdoor deployment. Subsequent work integrated optical filtering with adaptive digital algorithms to enable real-time background estimation and compensation under varying illumination, substantially extending operational light ranges[156]. Furthermore, methods based on background-light statistical modeling and hierarchical filtering combined with channel-aware compensation indicate that purely passive isolation is insufficient in dynamic environments[157,158], necessitating algorithmic enhancements. Overall, background suppression is evolving from passive filtering toward active sensing and adaptive compensation, providing crucial support for engineering VLC in complex outdoor scenarios.

Mobility introduces additional challenges in dynamic applications, such as vehicular communication, and wearable devices. Rapid changes in transceiver position and orientation can lead to beam misalignment or temporary link loss. In 2024, Pradhan et al. conducted a detailed analysis of frequency- and time-domain characteristics in mobile VLC, proposing an extended channel model for accurate dynamic channel estimation[159]. To enhance communication reliability under mobility, both algorithmic and hardware solutions are explored. Algorithmically, position-aware strategies have been proposed, dynamically adjusting or selecting optimal MIMO demultiplexing schemes based on

Fig. 13 | (a) Mobile visible light communication system. (b) Outdoor 100 m VLC system. (c) Kilometer-scale VLC system based on collimator. Figure reproduced with permission from: (a) ref.[161], under a Creative Commons License; (b) ref.[160], IEEE; (c) ref.[162], Optica Publishing Group.

real-time vehicle location information, as shown in Fig. 13(b)[160]. In 2024, Hou et al. demonstrated visual-aided positioning combined with dynamic optical-axis adjustment, using cameras to track transmitter location and motorized optics to quickly realign the beam, as shown in Fig. 13(a)[161]. At the hardware level, wide-FOV receiver designs can partially mitigate performance degradation caused by brief misalignment.

Compared with controlled lab environments, real-world channels are more complex and stochastic, affected by turbulence-induced scintillation, underwater scattering-induced multipath, and variable occlusions or shadowing. Such distortions are difficult to model accurately with fixed-parameter approaches. Recently, AI-driven end-to-end optimization has offered a new solution. Autoencoder-based communication frameworks jointly model coding, modulation, and channel compensation, learning optimal feature representations in a data-driven manner, thereby maintaining robustness under unknown or rapidly varying channels[101, 104]. Compared with traditional modular design, these methods exhibit superior adaptivity to complex channel impairments, providing effective tools for field-deployed systems.

Field trials have begun to validate VLC feasibility in real environments. For mid-to-short-range free-space links, Li et al. demonstrated an outdoor system achieving meter- to hundred-meter-scale transmission, systematically evaluating the effects of ambient light (day and night), receiver angle deviations, and environmental disturbances (rain, snow, fog) on bit-error performance[160], as shown in Fig. 13(b). High-power sources, optical focusing, and real-time equalization enabled stable transmission, providing key engineering references for outdoor deployment. For long-distance links, Dong et al. employed collimator, optimizing transmitter modules, broadband receivers, and real-time channel compensation to achieve near-laboratory performance. Stable transmission was maintained over an 8 km simulated distance at 7.64 Gbps[162], as illustrated in Fig. 13(c). In underwater VLC, Zhang et al. achieved 19.02 Gbps net rate over a

25 m pool using adaptive bit loading[38], while Lu et al. evaluated system performance under varying water quality (turbidity and salinity) and airflow disturbances, reaching 16.1 Gbps in pure water and maintaining 15.4 Gbps at 56 mg/L impurity concentration and 3 ppt salinity[119].

Overall, progressive field validations indicate that VLC has established a solid technical foundation for real-world deployment. Current experimental results closely follow the performance trends projected under ideal conditions (Fig. 3(b)). However, unlike laboratory benchmarks, practical deployments prioritize system stability, adaptivity, and engineering feasibility. Constructing intelligent VLC systems capable of dynamic sensing, autonomous adjustment, and multi-dimensional coordination is crucial for complex environments. Through the synergistic optimization of devices, algorithms, and system architectures, combined with long-term field testing, VLC is poised for scalable deployment in vehicular networks, marine communications, and space-based information networks.

6 Summary and perspective

Recent advances in visible light communication have achieved remarkable progress in transmission rate, link distance, and system robustness, establishing VLC as a promising candidate for future high-capacity wireless networks. This review has surveyed representative developments from three complementary perspectives, device technologies, signal processing algorithms, and system and network architectures, while highlighting the key challenges that continue to limit large-scale deployment. Building on these foundations, several forward-looking research directions are outlined below.

The first promising direction is perception-driven predictable communication and light-field modulation technology. Long-distance free space optical communication in the atmosphere and underwater faces turbulence interference, which causes signal attenuation and increased bit error rates in optical communication, thereby reducing the reliability of communication links. Existing turbulence assessment methods can only evaluate statistical turbulence intensity, failing to simultaneously capture instantaneous distorted wavefronts across non-coherent fields of view. Furthermore, classical turbulence compensation techniques rely solely on passive adjustments based on real-time wavefront measurements, lacking the ability to proactively predict and preemptively compensate for turbulence effects. Therefore, it is essential to explore adaptive optics technologies with multi-channel sensing fields to achieve spatial non-uniform turbulence sensing and prediction. Developing high-speed wavefront prediction algorithms enables proactive forecasting of dynamic turbulence, supporting more precise pre-compensation against turbulence to minimize its interference.

A second critical direction concerns the validation and deployment of VLC for inter-satellite and satellite-to-ground communications. Optical communication systems exhibit superior collimation due to higher antenna gains in transmission and reception compared to radio frequency antennas. The visible light band features shorter wavelengths and higher photon energy than infrared bands, resulting in lower beam divergence angles, wider device bandgaps, and stronger resistance to high-energy radiation interference. Integrating inter-satellite and satellite-to-ground visible light links with existing communication methods enables higher channel capacity and greater stability under adverse weather conditions, aligning with the future development direction of integrated space-air-ground-sea communication systems. It should be emphasized that the physical conditions in inter-satellite environments and satellite-to-ground communications differ fundamentally from those in terrestrial scenarios. Factors such as high relative velocities, frequent dynamic blockage, intense solar background radiation, and extreme low-temperature and high-radiation conditions impose much stricter requirements on channel modeling and CSI acquisition for visible light communication systems. Under these circumstances, conventional channel models based on statistical averaging or quasi-static assumptions may fail to accurately characterize link dynamics. Meanwhile, CSI estimation becomes more challenging due to rapid time variations and potential sampling latency. To address these issues, recent studies have increasingly explored data-driven approaches, incorporating deep learning frameworks and end-to-end autoencoder architectures to dynamically learn channel representations. Such methods enable real-time CSI prediction and adaptive signal compensation in fast-varying environments[13, 64], thereby enhancing the robustness and transmission efficiency of inter-satellite and satellite-to-ground visible light links.

The third major research frontier lies in visible-light photonic integration. High-speed visible light communication is currently constrained by device modulation bandwidth and electro-optic modulation efficiency. Additionally, the significantly shorter wavelengths of visible light signals compared to RF and infrared signals pose challenges in designing common components like external modulators and power dividers. Simultaneously, to enhance device integration, chips for high-speed VLC must exhibit good compatibility with traditional CMOS processes. Existing high-speed optical communication chips are primarily designed for the 1550 nm wavelength. In the visible spectrum, such devices currently lack precedents and robust design theories to support their development. Future research must therefore combine semiconductor design theory with computational numerical simulation to model visible light electro-optic and opto-electronic conversion processes. Meanwhile, materials with high bandwidth and high conversion efficiency must be identified for applications in visible-band frequency combs, external modulators, receivers.

In summary, the evolution of VLC is transitioning from isolated performance enhancement toward system-level intelligence, predictive adaptation, and chip-scale integration. Advances along these directions are expected to unlock new application scenarios, ranging from space communications and integrated sensing-communication systems to ultra-high-capacity optical interconnects, ultimately positioning VLC as a key enabling technology in future wireless networks.

References

1. Chi N, Zhou YJ, Wei YR et al. Visible light communication in 6G: advances, challenges, and prospects. *IEEE Veh Technol Mag* **15**, 93–102 (2020).
2. Chowdhury MZ, Shahjalal M, Ahmed S et al. 6G wireless communication systems: applications, requirements, technologies, challenges, and research directions. *IEEE Open J Commun Soc* **1**, 957–975 (2020).
3. Chi N, Haas H, Kavehrad M et al. Visible light communications: demand factors, benefits and opportunities [Guest Editorial]. *IEEE Wirel Commun* **22**, 5–7 (2015).
4. Pathak PH, Feng XT, Hu PF et al. Visible light communication, networking, and sensing: a survey, potential and challenges. *IEEE Commun Surv Tutorials* **17**, 2047–2077 (2015).
5. Elfikky A, Boghdady AI, Mumtaz S et al. Underwater visible light communication: recent advancements and channel modeling. *Opt Quantum Electron* **56**, 1617 (2024).
6. Oubei HM, Shen C, Kammoun A et al. Light based underwater wireless communications. *Jpn J Appl Phys* **57**, 08PA06 (2018).
7. Li FJ, Zhang HY, Lu ZL et al. Unsupervised learning enabled label-free single-pixel imaging for resilient information transmission through unknown dynamic scattering media. *Opto-Electron Adv* **8**, 250013 (2025).
8. Loureiro PA, Guiomar FP, Monteiro PP. Visible light communications: a survey on recent high-capacity demonstrations and digital modulation techniques. *Photonics* **10**, 993 (2023).
9. Pezeshki B, Khoeini F, Tselikov A et al. LED-array based optical interconnects for chip-to-chip communications with integrated CMOS drivers, detectors, and circuitry. *Proc SPIE* **12007**, 1200707 (2022).
10. Pezeshki B, Rangarajan S, Tselikov A et al. 304 channel MicroLED based CMOS transceiver IC with aggregate 1 Tbps and sub-pJ per bit capability. In *Proceedings of 2024 Optical Fiber Communications Conference and Exhibition (OFC)* 1–3 (IEEE, 2024). https://doi.org/10.1364/OFC.2024.M3A.1
11. Pezeshki B, Tselikov A, Kalman R et al. Micro-LED data interconnect for scale-up networks with record energy efficiency. In *Proceedings of 2025 IEEE Symposium on High-Performance Interconnects (HOTI)* 82–86 (IEEE, 2025). http://doi.org/10.1109/HOTI66940.2025.00026.
12. Amanor DN, Edmonson WW, Afghah F. Intersatellite communication system based on visible light. *IEEE Trans Aerosp Electron Syst* **54**, 2888–2899 (2018).
13. Alam A, Aziz AE, Basit A. A survey on inter-satellite links based on visible light communication. *Phys Commun* **72**, 102757 (2025).
14. Mohammed AS, Adnan SA, Ali MAA et al. Underwater wireless optical communications links: perspectives, challenges and recent trends. *J Opt Commun* **45**, 937–945 (2024).
15. Kaushal H, Kaddoum G. Underwater optical wireless communication. *IEEE Access* **4**, 1518–1547 (2016).
16. Zhou YJ, Lin XH, Xu ZY et al. Beyond 600 Gbps optical interconnect utilizing wavelength division multiplexed visible light laser communication [Invited]. *Chin Opt Lett* **23**, 050002 (2025).
17. Liu FL, Chen MA, Jiang WB et al. Effective auto-alignment and tracking of transceivers for visible-light communication in data centres. *Proc SPIE* **10945**, 109450N (2019).
18. Aletri OZ, Musa MOI, Alresheedi MT et al. Visible light optical data centre links. In *Proceedings of 2019 21st International Conference on Transparent Optical Networks (ICTON)* 1–5 (IEEE, 2019). http://doi.org/10.1109/ICTON.2019.8840517.
19. Karunatilaka D, Zafar F, Kalavally V et al. LED based indoor visible light communications: state of the art. *IEEE Commun Surv Tutorials* **17**, 1649–1678 (2015).
20. Mapunda GA, Ramogomana R, Marata L et al. Indoor visible light communication: a tutorial and survey. *Wireless Commun Mobile Comput* **2020**, 8881305 (2020).
21. Memedi A, Dressler F. Vehicular visible light communications: a survey. *IEEE Commun Surv Tutorials* **23**, 161–181 (2021).
22. Hasnawi RA, Marghescu I. A survey of vehicular VLC methodologies. *Sensors* **24**, 598 (2024).
23. Gupta S, Roy D, Bose S et al. Illuminating the future: a comprehensive review of visible light communication applications. *Opt Laser Technol* **177**, 111182 (2024).
24. Oubei HM, Duran JR, Janjua B et al. 4.8 Gbit/s 16-QAM-OFDM transmission based on compact 450-nm laser for underwater wireless optical communication. *Opt Express* **23**, 23302–23309 (2015).
25. Lee C, Shen C, Oubei HM et al. 2 Gbit/s data transmission from an unfiltered laser-based phosphor-converted white lighting communication system. *Opt Express* **23**, 29779–29787 (2015).
26. Shen C, Guo YJ, Oubei HM et al. 20-meter underwater wireless optical communication link with 1.5 Gbps data rate. *Opt Express* **24**, 25502–25509 (2016).
27. Kong MW, Lv WC, Ali T et al. 10-m 9.51-Gb/s RGB laser diodes-based WDM underwater wireless optical communication. *Opt Express* **25**, 20829–20834 (2017).
28. Wei LY, Hsu CW, Chow CW et al. 20.231 Gbit/s tricolor red/green/blue laser diode based bidirectional signal remodulation visible-light communication system. *Photonics Res* **6**, 422–426 (2018).
29. Wei LY, Chow CW, Hsu CW et al. Bidirectional visible light communication system using a single VCSEL with predistortion to enhance the upstream remodulation. *IEEE Photonics J* **10**, 7903407 (2018).
30. Wei LY, Hsu CW, Chow CW et al. 40-Gbit/s visible light communication using polarization-multiplexed R/G/B laser diodes with 2-m free-space transmission. In *Proceedings of 2019 Optical Fiber Communications Conference and Exhibition (OFC)* 1–3 (IEEE, 2019). https://doi.org/10.1364/OFC.2019.M3I.3
31. He J, Li ZQ, He J et al. Visible laser light communication based on LDPC-coded multi-band CAP and adaptive modulation. *J Lightwave Technol* **37**, 1207–1213 (2019).
32. Wang WC, Cheng CH, Wang HY et al. White-light color conversion with red/green/violet laser diodes and yellow light-emitting diode mixing for 34.8 Gbit/s visible lighting communication. *Photonics Res* **8**, 1398–1408 (2020).
33. Li GQ, Hu FC, Zou P et al. Beyond 10 Gbps 450-nm GaN laser diode based visible light communication system utilizing probabilistic shaping bit loading scheme. In *Proceedings of 2020 12th International Symposium on Communication Systems, Networks and Digital Signal Processing (CSNDSP)* 1–4 (IEEE, 2020). http://doi.org/10.1109/CSNDSP49049.2020.9249482.
34. Hu JH, Hu FC, Li GQ et al. A 15 Gbps 520-nm GaN laser diode based visible light communication system utilizing adaptive bit loading scheme. In *Proceedings of 2021 IEEE 6th Optoelectronics Global Conference (OGC)* 31–34 (IEEE, 2021).

http://doi.org/10.1109/OGC52961.2021.9654309.

35. Hu JH, Hu FC, Jia JL et al. 46.4 Gbps visible light communication system utilizing a compact tricolor laser transmitter. *Opt Express* **30**, 4365–4373 (2022).
36. Pahuja H, Sachdeva S, Sindhwani M. Capacity enhancement of WDM visible light communication system employing 3-SOPs/channel/LD color. *J Opt Commun* **46**, 107–113 (2025).
37. Li D, Ma CC, Wang JF et al. High-speed GaN-based superluminescent diode for 4.57 Gbps visible light communication. *Crystals* **12**, 191 (2022).
38. Zhang TY, Tian JH, Wang Y et al. 19.02Gbps/25m underwater wireless optical communication adopting probabilistic constellation shaping QAM-DMT transmission. In *Proceedings of 2023 Asia Communications and Photonics Conference/2023 International Photonics and Optoelectronics Meetings (ACP/POEM)* 1–4 (IEEE, 2023). http://doi.org/10.1109/ACP/POEM59049.2023.10369021.
39. Luo Z, Lin X, Lu Z et al. Over 100Gbps free-space laser-based visible light communication system based on 10-λ WDM module. In *Proceedings of the 49th European Conference on Optical Communications (ECOC 2023)* 980–983 (IET, 2023). http://doi.org/10.1049/icp.2023.2406.
40. Lin XH, Zhang HY, Lu ZL et al. 519.21 Gbps optical interconnect using 50-channel pre-equalized WDM visible light laser communication system. In *Proceedings of Optical Fiber Communication Conference 2024* Tu2K. 1 (Optica Publishing Group, 2024). http://doi.org/10.1364/OFC.2024.Tu2K.1.
41. Wang JF, Hu JH, Guan CW et al. High-speed GaN-based laser diode with modulation bandwidth exceeding 5 GHz for 20 Gbps visible light communication. *Photonics Res* **12**, 1186–1193 (2024).
42. Chi N, Niu WQ, Zhou YJ et al. Enabling technologies to achieve beyond 500 Gbps optical intra-connects based on WDM visible light laser communication. *J Lightwave Technol* **43**, 1843–1854 (2025).
43. Lu ZL, Liu XY, Wang YK et al. 831 Gbps optical interconnect for data centers based on PDM-WDM visible light communication system. In *Proceedings of 2025 23rd International Conference on Optical Communications and Networks (ICOCN)* 1–3 (IEEE, 2025). http://doi.org/10.1109/ICOCN67308.2025.11145642.
44. Hu JH, Jia HL, Gu ZQ et al. Investigation on large modulation bandwidth InGaN-based blue laser diodes. *Opt Laser Technol* **185**, 112601 (2025).
45. Issaoui L, Cho S, Chun H. High CRI RGB laser lighting with 11-Gb/s WDM link using off-the-shelf phosphor plate. *IEEE Photonics Technol Lett* **34**, 97–100 (2022).
46. Lee C, Zhang C, Cantore M et al. 4 Gbps direct modulation of 450 nm GaN laser for high-speed visible light communication. *Opt Express* **23**, 16232–16237 (2015).
47. Matthews W, Ahmed Z, Ali W et al. A 3.45 Gigabits/s SiPM-based OOK VLC receiver. *IEEE Photonics Technol Lett* **33**, 487–490 (2021).
48. Retamal JRD, Oubei HM, Janjua B et al. 4-Gbit/s visible light communication link based on 16-QAM OFDM transmission over remote phosphor-film converted white light by using blue laser diode. *Opt Express* **23**, 33656–33666 (2015).
49. Chi YC, Hsieh DH, Lin CY et al. Phosphorous diffuser diverged blue laser diode for indoor lighting and communication. *Sci Rep* **5**, 18690 (2015).
50. Lu ZL, Xu ZY, Zhou YN et al. 102.2 Gbps underwater visible light laser communication utilizing a tri-color laser transmitter and a neural network-based reverse signal generator. In *Proceedings of ECOC 2024; 50th European Conference on Optical Communication* 463–466 (VDE, 2024). https://ieeexplore.ieee.org/abstract/document/10926411
51. Lu ZL, Li ZH, Lin XH et al. 170 Gbps PDM underwater visible light communication utilizing a compact 5-λ laser transmitter and a reciprocal differential receiver. *Photonics Res* **13**, 1654–1665 (2025).
52. Wu TC, Chi YC, Wang HY et al. Blue laser diode enables underwater communication at 12.4 Gbps. *Sci Rep* **7**, 40480 (2017).
53. Gunawan WH, Liu Y, Chow CW et al. High speed visible light communication using digital power domain multiplexing of orthogonal frequency division multiplexed (OFDM) signals. *Photonics* **8**, 500 (2021).
54. Luo ZT, Lin XH, Lu ZL et al. 113 Gbps rainbow visible light laser communication system based on 10λ laser WDM emitting module in fiber-free space-fiber link. *Opt Express* **32**, 2561–2573 (2024).
55. Chun H, Gomez A, Quintana C et al. A wide-area coverage 35 Gb/s visible light communications link for indoor wireless applications. *Sci Rep* **9**, 4952 (2019).
56. Chi YC, Hsieh DH, Tsai CT et al. 450-nm GaN laser diode enables high-speed visible light communication with 9-Gbps QAM-OFDM. *Opt Express* **23**, 13051–13059 (2015).
57. Fei C, Hong XJ, Zhang GW et al. 16.6 Gbps data rate for underwater wireless optical transmission with single laser diode achieved with discrete multi-tone and post nonlinear equalization. *Opt Express* **26**, 34060–34069 (2018).
58. Fei C, Zhang JW, Zhang GW et al. Demonstration of 15-M 7.33-Gb/s 450-nm underwater wireless optical discrete multitone transmission using post nonlinear equalization. *J Lightwave Technol* **36**, 728–734 (2018).
59. Huang YF, Chi YC, Kao HY et al. Blue laser diode based free-space optical data transmission elevated to 18 Gbps over 16 m. *Sci Rep* **7**, 10478 (2017).
60. Lu ZL, Cai JF, Xu ZY et al. 11.2 Gbps 100-meter free-space visible light laser communication utilizing bidirectional reservoir computing equalizer. *Opt Express* **31**, 44315–44327 (2023).
61. Zhou YN, Lu ZL, Wang YK et al. Beyond 50 Gbps 100 m visible light laser communication single-transmitter-multi-receiver system utilizing triple branch neural network. *Opt Express* **33**, 18378–18392 (2025).
62. Oyewobi SS, Djouani K, Kurien AM. Visible light communications for internet of things: prospects and approaches, challenges, solutions and future directions. *Technologies* **10**, 28 (2022).
63. Najda SP, Perlin P, Suski T et al. GaN laser diode technology for visible-light communications. *Electronics* **11**, 1430–1430 (2022).
64. Saxena VN, Dwivedi VK, Gupta J. Machine learning in visible light communication system: a survey. *Wireless Commun Mobile Comput* **2023**, 3950657 (2023).
65. He CW, Chen C. A review of advanced transceiver technologies in visible light communications. *Photonics* **10**, 648 (2023).
66. Sejan MAS, Rahman MH, Aziz MA et al. A comprehensive survey on MIMO visible light communication: current research, machine learning and future trends. *Sensors* **23**, 739 (2023).
67. Liang CX, Li JR, Liu SC et al. Integrated sensing, lighting and communication based on visible light communication: a review. *Digit Signal Process* **145**, 104340 (2024).
68. Sikder P, Rahman MT, Bakibillah ASM. Advancements and challenges of visible light communication in intelligent transportation systems: a comprehensive review. *Photonics* **12**, 225 (2025).
69. Jayaweera VL, Peiris C, Darshani D et al. Visible light communication for underwater applications: principles, challenges, and future prospects. *Photonics* **12**, 593 (2025).
70. Li XY, Cheng C, Zhang C et al. Net 4 Gb/s underwater optical wireless communication system over 2 m using a single-pixel GaN-based blue mini-LED and linear equalization. *Opt Lett* **47**, 1976–1979 (2022).
71. Li ZH, Zhang XR, Hao ZB et al. Bandwidth analysis of high-speed InGaN micro-LEDs by an equivalent circuit model. *IEEE Electron*

Device Lett **44**, 785–788 (2023).
72. Xu ZY, Niu WQ, Liu Y et al. 31.38 Gb/s GaN-based LED array visible light communication system enhanced with V-pit and sidewall quantum well structure. *Opto-Electron Sci* **2**, 230005 (2023).
73. Jia HL, Hu JH, Xu ZY et al. High-speed blue laser diodes with InGaN quantum barrier for beyond 36 Gbps visible light communications. *Laser Photon Rev* **19**, 2401751 (2025).
74. Li ZH, Xu ZY, Li SQ et al. 21.79/17.49 Gbps full-duplex visible light communication enabled by short-cavity blue and green InGaN/GaN laser diodes. *J Lightwave Technol* **43**, 3348–3357 (2025).
75. Xu ZY, Luo ZT, Lin XH et al. 15.26Gb/s Si-substrate GaN high-speed visible light photodetector with super-lattice structure. *Opt Express* **31**, 33064–33076 (2023).
76. Xu ZY, Lin XH, Luo ZT et al. Flexible 2 × 2 multiple access visible light communication system based on an integrated parallel GaN/InGaN micro-photodetector array module. *Photonics Res* **12**, 793–803 (2024).
77. Jung W. *Op Amp Applications Handbook* (Newnes, Burlington, 2005).
78. Milovančev D, Jukić T, Vokić N et al. VLC using 800-μm diameter APD receiver integrated in standard 0.35-μm BiCMOS technology. *IEEE Photonics J* **13**, 7900513 (2021).
79. Fei C, Wang Y, Du J et al. 100-m/3-Gbps underwater wireless optical transmission using a wideband photomultiplier tube (PMT). *Opt Express* **30**, 2326–2337 (2022).
80. Chen JY, Ren Y, Long F et al. An adaptive threshold updating algorithm for PMT-based ultraviolet communication. *IEEE Photonics J* **17**, 7301210 (2025).
81. Huang SJ, Li YC, Chen C et al. Performance analysis of SPAD-based optical wireless communication with OFDM. *J Opt Commun Networking* **15**, 174–186 (2023).
82. Huang J, Li CK, Dai JS et al. Real-time and high-speed underwater photon-counting communication based on SPAD and PPM symbol synchronization. *IEEE Photonics J* **13**, 7300209 (2021).
83. Seminara M, Nawaz T, Caputo S et al. Characterization of field of view in visible light communication systems for intelligent transportation systems. *IEEE Photonics J* **12**, 7903816 (2020).
84. Ye ZW, Zhang YY, Wang C et al. RIS-aided dynamically adaptive wide field-of-view receiver for visible light communication in industrial internet of things. *Opt Express* **31**, 34748–34763 (2023).
85. Shi JY, Xu ZY, Niu WQ et al. Si-substrate vertical-structure InGaN/GaN micro-LED-based photodetector for beyond 10 Gbps visible light communication. *Photonics Res* **10**, 2394–2404 (2022).
86. Xu ZY, Luo ZT, Lin XH et al. A novel hybrid detection scheme for visible light broadcast communication and dedicated communication based on a GaN detector array. *J Lightwave Technol* **43**, 3171–3182 (2025).
87. Dai SJ, Xu ZY, Qian WF et al. Quasi-2D perovskite luminescent solar concentrators enable large field-of-view and high-speed visible light communication. *ACS Appl Mater Interfaces* **17**, 51212–51219 (2025).
88. Batista AAC, Amorim TD, Ribeiro RM et al. Enhanced photodetector field of view for IoT-driven VLC systems using fluorescent optical antennas. *IEEE Access* **13**, 134955–134965 (2025).
89. Lin XH, Yang P, Li JL et al. 120° field-of-view CsPbBr3 quantum dots fluorescent antenna for visible light communication beyond 1 Gbps. In *Proceedings of 2025 30th OptoElectronics and Communications Conference (OECC) and 2025 International Conference on Photonics in Switching and Computing (PSC)* 1–4 (IEEE, 2025). http://doi.org/10.23919/OECC/PSC62146.2025.11111023.
90. Chi N, Zhou YJ, Liang SY et al. Enabling technologies for high-speed visible light communication employing CAP modulation. *J Lightwave Technol* **36**, 510–518 (2018).
91. Wang Z, Chen J, Chi N. A novel algorithm for improving the spectrum efficiency of non-orthogonal multiband CAP UVLC systems. *J Lightwave Technol* **38**, 6187–6201 (2020).
92. Lin XH, Zhang HY, Niu WQ et al. Faster-than-Nyquist *N*-dimensional CAP modulation scheme based on slicing sphere decoder for visible light communication. *J Lightwave Technol* **42**, 8713–8729 (2024).
93. Nie YG, Chen C, Zeng ZH et al. Interference mitigation for faster-than-Nyquist *m*CAP in bandlimited VLC: a low-complexity gapped index modulation approach. *J Lightwave Technol* **43**, 6533–6546 (2025).
94. Lin XH, Wang ZC, Zhou YJ et al. Flexible multi-access scheme for indoor VLC using multiband N-dimensional CAP and a wide field-of-view white laser transmitter. *Opt Express* **33**, 4194–4210 (2025).
95. Zhang YZ, Liu XQ, Chen JQ et al. An enhanced bit loading scheme with pairwise coding for low-pass VLC systems. In *Proceedings of ICC 2023 - IEEE International Conference on Communications* 3308–3313 (IEEE, 2023). http://doi.org/10.1109/ICC45041.2023.10279453.
96. Yaseen M, Canbilen AE, Ikki S. Channel estimation in visible light communication systems: the effect of input signal-dependent noise. *IEEE Trans Veh Technol* **72**, 14330–14340 (2023).
97. Wu X, Huang ZT, Ji YF. Deep neural network method for channel estimation in visible light communication. *Opt Commun* **462**, 125272 (2020).
98. Gao ZP, Wang YH, Liu XD et al. FFDNet-based channel estimation for massive MIMO visible light communication systems. *IEEE Wirel Commun Lett* **9**, 340–343 (2020).
99. Rahman MH, Chowdhury MZ, Utama IBKY et al. Channel estimation for indoor massive MIMO visible light communication with deep residual convolutional blind denoising network. *IEEE Trans Cogn Commun Netw* **9**, 683–694 (2023).
100. Liu SC, Mou YN, Zhang H. Block-sparse learning enabled approach towards efficient channel estimation for underwater visible light communications. In *Proceedings of 2024 International Wireless Communications and Mobile Computing (IWCMC)* 1166–1170 (IEEE, 2024). http://doi.org/10.1109/IWCMC61514.2024.10592451.
101. Cai JF, Li ZW, Chi N. Physical prior inspired ensemble learning enables effective channel estimation of underwater visible light communication. *Opt Express* **31**, 16148–16161 (2023).
102. Wei Y, Chen CX, Li FJ et al. An accurate and realistic channel simulator of optical wireless communication systems combining deterministic and random noise. *J Lightwave Technol* **42**, 2666–2682 (2024).
103. Jin RZ, Wei Y, Zhang JW et al. Neural-network-based end-to-end learning for adaptive optimization of two-dimensional signal generation in UVLC systems. *Opt Express* **32**, 6309–6328 (2024).
104. Shi JY, Niu WQ, Li ZW et al. Optimal adaptive waveform design utilizing an end-to-end learning-based pre-equalization neural network in an UVLC system. *J Lightwave Technol* **41**, 1626–1636 (2023).
105. Chen JY, Jiang M. Joint blind channel estimation, channel equalization, and data detection for underwater visible light communication systems. *IEEE Wirel Commun Lett* **10**, 2664–2668 (2021).
106. Zhang HY, Chen CX, Li FJ et al. Single-pass wavefront reconstruction via depth heterogeneity self-supervised neural operator for turbulence correction. *Laser Photon Rev* **19**, e00909 (2025).
107. Sun SY, Yang F, Mei WD et al. Channel estimation for optical intelligent reflecting surface-assisted VLC system: a joint space-time sampling approach. *IEEE J Sel Areas Commun* **43**, 867–882 (2025).
108. Fujimoto N, Mochizuki H. 477 Mbit/s visible light transmission based on OOK-NRZ modulation using a single commercially avail-

able visible LED and a practical LED driver with a pre-emphasis circuit. In *Proceedings of National Fiber Optic Engineers Conference 2013* JTh2A. 73 (Optica Publishing Group, 2013). https://doi.org/10.1364/NFOEC.2013.JTh2A.73.

109. Huang XX, Chen SY, Wang ZX et al. 2.0-Gb/s visible light link based on adaptive bit allocation OFDM of a single phosphorescent white LED. *IEEE Photonics J* **7**, 7904008 (2015).
110. Huang XX, Shi JY, Li JH et al. A Gb/s VLC transmission using hardware preequalization circuit. *IEEE Photonics Technol Lett* **27**, 1915–1918 (2015).
111. Zhang XD, Hu ZR, Feng Z et al. Nonlinearity mitigation in a 32APSK visible light communication system utilizing windowed single carrier frequency domain equalization. In *Proceedings of 2025 23rd International Conference on Optical Communications and Networks (ICOCN)* 1–3 (IEEE, 2025). http://doi.org/10.1109/ICOCN67308.2025.11145450.
112. Chen ZW, Lu ZL, Zhang XD et al. 39.54 Gbps underwater visible light communication utilizing a distributed equalizer and dual-polarization receiver. In *Proceedings of 2025 23rd International Conference on Optical Communications and Networks (ICOCN)* 1–3 (IEEE, 2025). http://doi.org/10.1109/ICOCN67308.2025.11145354.
113. Zhang HY, Yang AY, Xu H et al. 16QAM-OFDM VLC system based on frequency domain precompensation and DNN post-equalization. *IEEE Internet Things J* **12**, 12278–12286 (2025).
114. Khawatmi A, Saeed N, Atef M. Real-time single-channel 500 Mb/s visible light communication using pre-equalizer and LMS adaptive post-equalization. *Opt Laser Technol* **192**, 114082 (2025).
115. Zhao YH, Zou P, Shi M et al. Nonlinear predistortion scheme based on Gaussian kernel-aided deep neural networks channel estimator for visible light communication system. *Opt Eng* **58**, 116108 (2019).
116. Zhou YJ, Wei YR, Hu FC et al. Comparison of nonlinear equalizers for high-speed visible light communication utilizing silicon substrate phosphorescent white LED. *Opt Express* **28**, 2302–2316 (2020).
117. Hu FC, Holguin-Lerma JA, Mao Y et al. Demonstration of a low-complexity memory-polynomial-aided neural network equalizer for CAP visible-light communication with superluminescent diode. *Opto-Electron Adv* **3**, 200009 (2020).
118. Lu XY, Li Y, Chen X et al. Discrete wavelet transform assisted convolutional neural network equalizer for PAM VLC system. *Opt Express* **32**, 10429–10443 (2024).
119. Lu ZL, Li FJ, Cai JF et al. Turbulence resistant dual-aperture receiver with a sparse dual-polarization triple-branch network in underwater visible light communication. *J Lightwave Technol* **43**, 7663–7675 (2025).
120. Niu WQ, Xu ZY, Liu Y et al. Key technologies for high-speed si-substrate LED based visible light communication. *J Lightwave Technol* **41**, 3316–3331 (2023).
121. Jamali MV, Mirani A, Parsay A et al. Statistical studies of fading in underwater wireless optical channels in the presence of air bubble, temperature, and salinity random variations. *IEEE Trans Commun* **66**, 4706–4723 (2018).
122. Baykal Y. Scintillation index in strong oceanic turbulence. *Opt Commun* **375**, 15–18 (2016).
123. Jiang HY, Qiu HB, He N et al. Performance of spatial diversity DCO-OFDM in a weak turbulence underwater visible light communication channel. *J Lightwave Technol* **38**, 2271–2277 (2020).
124. Hu ZR, Zhang XD, Feng Z et al. Turbulence-resilient visible light communication system utilizing NLTCP coding and polarization multiplexing reception. In *Proceedings of 2025 30th OptoElectronics and Communications Conference (OECC) and 2025 International Conference on Photonics in Switching and Computing (PSC)* 1–4 (IEEE, 2025). http://doi.org/10.23919/OECC/PSC62146.2025.11111173.
125. Feng Z, Chen ZW, Lu ZL et al. 73.31-Gbps 5-m underwater visible light communication system utilizing a 5-λ laser transmitter and a polarization-diverse dual-aperture receiver. *Chin Opt Lett* **23**, 120603 (2025).
126. Wang ZL, Mu XD, Liu YW. Beamfocusing optimization for near-field wideband multi-user communications. *IEEE Trans Commun* **73**, 555–572 (2025).
127. Xing Z, Wang R, Yuan XJ. Joint active and passive beamforming design for reconfigurable intelligent surface enabled integrated sensing and communication. *IEEE Trans Commun* **71**, 2457–2474 (2023).
128. Liu C, Yuan WJ, Li SY et al. Learning-based predictive beamforming for integrated sensing and communication in vehicular networks. *IEEE J Sel Areas Commun* **40**, 2317–2334 (2022).
129. Liu ZH, Yang F, Song J et al. NOMA-based MISO visible light communication systems with optical intelligent reflecting surface: joint active and passive beamforming design. *IEEE Internet Things J* **11**, 18753–18767 (2024).
130. Ye YQ, Lian DX, Chen ZS et al. Visible-light optical phased array on a thin-film lithium niobate platform for high-speed beam steering. *Opt Lett* **50**, 3090–3093 (2025).
131. Ma XY, Yuan MR, Li JC et al. Multi-target and ultra-high-speed optical wireless communication using a thin-film lithium niobate optical phased array. *Nat Commun* **17**, 969 (2025).
132. Yue GC, Li Y. Integrated lithium niobate optical phased array for two-dimensional beam steering. *Opt Lett* **48**, 3633–3636 (2023).
133. Niu WQ, Li FJ, Xu ZY et al. Wavelength-multiplexed beam steering in fiber and visible light communication integrated indoor access network. In *Proceedings of Optical Fiber Communication Conference (OFC) 2024* Tu2K. 8 (Optica Publishing Group, 2024). http://doi.org/10.1364/OFC.2024.Tu2K.8.
134. Li FJ, Zhang HY, Lu ZL et al. 167Gbps 1×16 programmable visible light optical switching for data center optical interconnects. In *Proceedings of Optical Fiber Communication Conference (OFC) 2025* W4D. 4 (Optica Publishing Group, 2025). http://doi.org/10.1364/OFC.2025.W4D.4.
135. Lin QX, Fang SC, Yu Y et al. Optical multi-beam steering and communication using integrated acousto-optics arrays. *Nat Commun* **16**, 4501 (2025).
136. Wang XM, Ji PR, Zhang Z et al. Chip-scale optical phased array for broadband two-dimensional beam steering at visible wavelengths. *Opt Laser Technol* **181**, 111615 (2025).
137. Sun SY, Mei WD, Yang F et al. Optical intelligent reflecting surface assisted MIMO VLC: channel modeling and capacity characterization. *IEEE Trans Wirel Commun* **23**, 2125–2139 (2024).
138. Zhu JA, Gu Z, Ma Q et al. A self-controlled reconfigurable intelligent surface inspired by optical holography. *Nat Electron* **8**, 1108–1118 (2025).
139. Wang WH, Tan YJ, Tan TC et al. On-chip topological beamformer for multi-link terahertz 6G to XG wireless. *Nature* **632**, 522–527 (2024).
140. Hu JH, Guo ZY, Shi JY et al. A metasurface-based full-color circular auto-focusing Airy beam transmitter for stable high-speed underwater wireless optical communications. *Nat Commun* **15**, 2944 (2024).

141. Benyahya K, Diaz AG, Liu JY et al. Mosaic: breaking the optics versus copper trade-off with a wide-and-slow architecture and MicroLEDs. In *Proceedings of the ACM SIGCOMM 2025 Conference* 234–247 (ACM, 2025). https://doi.org/10.1145/3718958.3750510.
142. Wei WT, Gu HX, Wang K et al. Multi-dimensional resource allocation in distributed data centers using deep reinforcement learning. *IEEE Trans Network Serv Manage* **20**, 1817–1829 (2023).
143. Yang HN, Wilkinson P, Robertson B et al. 24 [1×12] wavelength selective switches integrated on a single 4k LCoS device. *J Lightwave Technol* **39**, 1033–1039 (2021).
144. Li FJ, Lu ZL, Zhang HY et al. 629Gbps wavelength-multiplexed 1 × 16 programmable visible light optical switching for data center optical interconnects. *J Lightwave Technol* **43**, 7692–7706 (2025).
145. Wu Y, Chen J, Wang Y et al. Tbps wide-field parallel optical wireless communications based on a metasurface beam splitter. *Nat Commun* **15**, 7744 (2024).
146. Sun AL, Xing SZ, Deng XY et al. Edge-guided inverse design of digital metamaterial-based mode multiplexers for high-capacity multi-dimensional optical interconnect. *Nat Commun* **16**, 2372 (2025).
147. Yuan Y, Peng YW, Sorin WV et al. A 5 × 200 Gbps microring modulator silicon chip empowered by two-segment Z-shape junctions. *Nat Commun* **15**, 918 (2024).
148. PittalàF, Braun RP, Böcherer G et al. 1.71 Tb/s single-channel and 56.51 Tb/s DWDM transmission over 96.5 km field-deployed SSMF. *IEEE Photonics Technol Lett* **34**, 157–160 (2022).
149. Shi JY, Fang XY, Niu WQ et al. 800 Gbps visible light communication system employing WDM and OAM multiplexing. In *Proceedings of 2022 20th International Conference on Optical Communications and Networks (ICOCN)* 1–3 (IEEE, 2022). http://doi.org/10.1109/ICOCN55511.2022.9901298.
150. Buzaverov KA, Baburin AS, Sergeev EV et al. Silicon nitride integrated photonics from visible to mid-infrared spectra. *Laser Photon Rev* **18**, 2400508 (2024).
151. Poon JKS, Govdeli A, Sharma A et al. Silicon photonics for the visible and near-infrared spectrum. *Adv Opt Photonics* **16**, 1–59 (2024).
152. Hulyal SU, Hu JQ, Wang CL et al. Arrayed waveguide gratings in lithium tantalate integrated photonics. *Optica* **12**, 978–984 (2025).
153. Zhang D, Cui YH, Cao XW et al. Integrated sensing and communications over the years: an evolution perspective. *IEEE Commun Surv Tutorials* **28**, 5014–5048 (2026).
154. Mohsan SAH, Qian HZ, Amjad H. A comprehensive review of optical wireless power transfer technology. *Front Inf Technol Electron Eng* **24**, 767–800 (2023).
155. Adiono T, Pradana A, Putra RVW et al. Analog filters design in VLC analog front-end receiver for reducing indoor ambient light noise. In *Proceedings of 2016 IEEE Asia Pacific Conference on Circuits and Systems (APCCAS)* 581–584 (IEEE, 2016). http://doi.org/10.1109/APCCAS.2016.7804058.
156. Umair MA, Meucci M, Catani J. Strong noise rejection in VLC links under realistic conditions through a real-time SDR front-end. *Sensors* **23**, 1594 (2023).
157. Sindhubala K, Vijayalakshmi B. Simulation of VLC system under the influence of optical background noise using filtering technique. *Mater Today: Proc* **4**, 4239–4250 (2017).
158. Patel PN, Dann J. Performance and design analysis of visible light communication systems amidst optical background noise utilizing filtering techniques. In Gupta D, Kamble V, Satpute V et al. *Paradigm Shifts in Communication, Embedded Systems, Machine Learning, and Signal Processing* 232–242 (Springer Cham, 2025). https://doi.org/10.1007/978-3-031-90577-3_21.
159. Pradhan J, Kappala VK, Majhi S et al. Time-varying channel estimation for ACO-OFDM VLC over mobile environment. *IEEE Trans Veh Technol* **73**, 11556–11567 (2024).
160. Li GQ, Niu WQ, Ha YNE et al. Position-dependent MIMO demultiplexing strategy for high-speed visible light communication in internet of vehicles. *IEEE Internet Things J* **9**, 10833–10850 (2022).
161. Hou YQ, Wang ZC, Li ZX et al. Laser-based mobile visible light communication system. *Sensors* **24**, 3086 (2024).
162. Dong F, Luo ZT, Xu ZY et al. Multi-kilometer visible light communication utilizing nonlinearity-adaptive hybrid probabilistic-geometric shaping. *Opt Express* **32**, 31699–31713 (2024).

Acknowledgements

We are grateful for financial supports from the Natural Science Foundation of China Project (No. 62525102).

Author contributions

N. Chi and Z. L. Lu conceived the scope and framework of the review. Z. L. Lu performed the literature search and classification. Z. L. Lu, F. J. Li, H. Y. Zhang, Y. K. Wang, X. Y. Liu, Z. W. Chen, Z. Feng and Z. R. Hu wrote the original draft. Z. W. Li, C. Shen, J. W. Zhang, Z. X. He, and N. Chi gave feedback on editing this manuscript. All authors reviewed and revised the manuscript and approved the final version.

Competing interests

The authors declare no competing financial interests.

Published by Editorial Office of *Opto-Electronic Technology*, Institute of Optics and Electronics, Chinese Academy of Sciences.

Opto-Electronic Journals Group
www.oejournal.org

Scan for Article PDF